Neural Adaptation and Instability in the Mammalian Retina

By

Jacob Khoussine

A dissertation submitted in partial fulfillment of

the requirements for the degree of

Doctor of Philosophy

(Cell and Molecular Biology)

at the

UNIVERSITY OF WISCONSIN-MADISON

2025

Date of final oral examination: 3/7/2025

The dissertation is approved by the following members of the Final Oral Committee:
Mrinalini Hoon, Associate Professor, Ophthalmology & Visual Sciences
Raunak Sinha, Associate Professor, Neuroscience
Elizabeth Felton, Assistant Professor, Neurology
Anjon Audhya, Professor, Biomolecular Chemistry
David Gamm, Professor, Ophthalmology & Visual Sciences

Abstract

Neural circuits can withstand moderate disruptions and still function, but there comes a threshold beyond which plasticity falters and networks collapse. This thesis investigates that boundary in the visual system using the mammalian retina as a model, revealing how neural circuits adapt to disruption and what occurs when their resilience is exceeded. Chapter 1 describes how light-driven activity and synaptic adjustments shape visual circuits early in life and how these adaptive processes preserve function in response to progressive input loss throughout life. Chapter 2 focuses on two mouse models of congenital stationary night blindness (CSNB) with either ~50% or 100% loss of ON pathway input. We used patch-clamp electrophysiology to record the intrinsic properties, synaptic inputs, and spike outputs of retinal ganglion cells, combined with single-cell immunohistochemistry to assess dendritic synapse composition, and contextualized these findings with assays of visual behavior in each model. Partial loss triggers structural adjustments that maintain signal output, whereas complete suppression overwhelms the circuit's capacity to adapt, leading to intrinsic changes and destabilizing bursts of aberrant activity. This contrast reveals a tipping point at which plasticity-driven alterations fail to preserve function. Chapter 3 examines how emerging retinal imaging methods and gene therapies might detect and correct such imbalances before they reach this critical threshold. Ultimately, the unifying theme of this thesis is that understanding visual neuroplasticity in health and disease is fundamental to preserving and restoring vision.

Acknowledgements

This work, and the substantial growth I've experienced in carrying it out, would have been impossible without the concentrated efforts of my family, teachers, and colleagues.

To my parents, thank you for believing in me and giving me the freedom to explore, stumble, and grow. My father's quiet strength and relentless dedication to creating opportunities he never had have fueled my own ambition. Mom, you tempered that ambition with warmth and laughter, reminding me of the power of our words and actions. Your resilience and steadfast support have been the foundation of my success. To my siblings, Michaela and Elias, I hope you are as proud of me as I am of you.

To the teachers who sparked my curiosity—Ms. Debbie Adams, thank you for recognizing my potential and inviting me to *Neuro Night*. I can still picture myself running to our minivan wearing a paper white coat and telling my mom I wanted to be a brain doctor. Dr. Douglas Gaffin, you introduced me to a passion for experimentation and sensory neuroscience. The first time I heard the crackling of action potentials in a neural recording, I knew that I wanted to be a neurophysiologist. Dr. James Thompson, you showed me that research is both art and science, encouraging me to approach experiments and communication with creativity. To the ENDURE neuroscience program, thank you for opening doors I didn't know existed. Without programs like yours, I may never have found the MD/PhD path.

A defining part of my graduate training has been the interplay between research and clinical experiences. In the inherited retinal degeneration clinic, Dr. Kimberley Stepien showed me how to support and bring hope to people experiencing progressive vision loss. It opened my eyes to the bottlenecks in translating scientific ideas from the lab to patients and invigorated me to understand how to treat those bottlenecks. Dr. Dave Gamm showed me the type of physician-scientist I aspire to be through the trust and connection he fosters with patients and their families. By working in the pediatric ophthalmology clinic with Dr. Gamm, I gained a practical sense for neuroplasticity in the prevention of amblyopia, an idea woven throughout this work. These experiences went

beyond observation; they shaped my identity as a scientist, pushing me to consider how research translates into patient care and the challenges along that path.

To my colleagues and mentors, I am deeply grateful. I remember walking into Dr. Raunak Sinha's lab when he was building his first electrophysiology rig. Several rigs and 10+ trainees later, the Sinha Lab is a well-oiled machine of retinal neurophysiology, and I'm grateful to have had the chance to learn from your expertise during my time in the Hoon Lab. Special thanks to Abhilash Sawant who spent countless hours saving me from trouble and teaching me to troubleshoot.

Thank you to the MD/PhD program for the opportunity to pursue this dream. You provided the resources to become a thoughtful physician-scientist and the flexibility to lean into my interests as I designed my own education. To Dr. Elizabeth Felton, thank you for being on my committee, and for spearheading the creation of the UW MSTP Summer Scholar Program. Working with the scholars in this program fulfilled me and allowed me to give back the support that was so critical for me to get to this point.

At its core, this thesis is about how systems endure strain until they reach their limits. This brings me to Dr. Mrinalini Hoon, who is the personification of plasticity. She does not believe in sink or swim; she believes in lifting people up. Watching her build her lab from the ground up, endure her own setbacks, and push onward and upward has been one of the greatest joys of my training. She has created a lab full of smart, kind, and motivated people exploring the cutting edge of retinal neurobiology. Mrinalini is continually engaged with her trainee's projects, and she approaches each trainee as the individual they are. Because of Mrinalini's support, I pushed with my limits without ever finding them, allowing me to grow as a person. She kept the magic of science alive, and I could not have imagined a better scientific and personal match for a thesis advisor.

Table of Contents

Abbreviation List

AII, AII amacrine cell
AMPA, α-amino-3-hydroxy-5-methyl-4-isoxazolepropionic acid
AOSLO, adaptive optics scanning light ophthalmoscopy
APB, 2-amino-4-phosphonobutyric acid (aka L-AP-4)
CPPG, cyclopropyl-4-phosphonophenylglycine
CSNB, complete congenital stationary night blindness
ERG, electroretinogram
GABA, gamma-aminobutyric acid
GlyRa1, glycine receptor alpha 1
GRM6, glutamate receptor metabotropic 6 (gene)
HET, heterozygous
IPL, inner plexiform layer
KO, knockout
LGN, lateral geniculate nucleus
LTD, long-term depression
LTP, long-term potentiation
mGluR6, metabotropic glutamate receptor 6
OCT, optical coherence tomography
OMR, optomotor response
OPL, outer plexiform layer
ORG, optoretinography
PSD95, postsynaptic density protein 95
R*/rod/sec, rhodopsin isomerizations per rod per second
R*/cone/sec, cone opsin isomerizations per cone per second
RGC, retinal ganglion cell
RP, retinitis pigmentosa
sEPSC, spontaneous excitatory postsynaptic current
WT, wildtype

Chapter 1: Background

A newborn enters the world with an immature visual system. Initially, its vision is dull and blurred because the neural circuits responsible for high-definition vision require light-driven activity to sculpt pathways to maturity (Mauer and Lewis, 2001). As light passes through the newborn's eyes, the concert begins in the retina—a thin, transparent sheet of neural tissue lining the back of the eye. Photons strike photoreceptors like fingers on piano keys, generating patterns of electrical signals that travel through the retina. These signals exit each eye via the optic nerves, pass through the thalamus, and reach the visual cortex, where perception emerges. With each wave of light-driven impulses, the structural and functional architecture of visual circuits becomes refined (Katz and Shatz, 1996). By 2 to 3 years of age, the infant's vision clarifies into the full panoply of color, contrast, motion, and luminance that compose our visual scenes.

Visual information is first processed within the retina, where photoreceptors initiate signal transformation. These neurons fall into two classes: rods and cones. Rod photoreceptors are exceptionally sensitive and can detect single photons to enable night vision. Cone photoreceptors specialize in color and high-acuity vision but require brighter light for activation. Humans express three cone subtypes, each tuned to different wavelengths—red, green, or blue—ensuring distinct spectral information is preserved as signals travel through the visual system. When cone subtypes are absent, as seen in red-green color blindness, critical information is lost, leaving the visual cortex with an incomplete message and impaired color perception (Neitz and Neitz, 2000).

Central to the fidelity of visual information transfer is the synapse, the site where neurons communicate with each other. In the retina, synapses consist of axon terminals of presynaptic neurons and dendrites of postsynaptic neurons, which together form a compartment for synaptic output and input, respectively. High-fidelity transmission relies on the integrity of these input-output relationships. Synaptic plasticity, particularly early in life, allows these connections to refine dynamically in response to visual experience, tuning circuits for stability throughout life.

Visual computations unfold across two synaptic layers in the retina. The outer plexiform layer (OPL) forms a three-way junction between photoreceptors, bipolar cells, and horizontal cells (Hoon et al, 2014). Photoreceptors communicate via specialized ribbon synapses, which sustain continuous neurotransmitter release, facilitating rapid and graded transmission of glutamate in response to changing light conditions. Horizontal cells provide reciprocal feedback to photoreceptors, which can be through several species-specific mechanisms, fine-tuning photoreceptor output to enhance signal transmission (Kramer and Davenport, 2015). Bipolar cells relay photoreceptor signals, diverging into rod bipolar cells, which process dim-light increments via the ON pathway, and cone bipolar cells, which subdivide into ON and OFF pathways—activating in response to bright-light increments or decrements, respectively (Wassel, 2004). Note that the ON pathway is molecularly defined through expression of the metabotropic glutamate receptor, mGluR6, at bipolar cell dendrites, while the OFF bipolar cells express AMPA/kainate glutamate receptors. This functional division expands the retina’s dynamic operating range, ensuring sensitivity across varying light conditions.

Deeper in the retina, the inner plexiform layer (IPL) forms another tripartite junction, this time involving bipolar cells, amacrine cells, and ganglion cells (Fig 1). The IPL is divided into ON and OFF sublayers, preserving the signal segregation initiated in the OPL. Amacrine cells are GABAergic or glycinergic inhibitory interneurons that play diverse roles in refining visual signals. Some, like the AII amacrine cell, facilitate crosstalk between ON and OFF pathways to regulate OFF bipolar and ganglion cell responses (Manookin et al, 2008). Others, such as the starburst amacrine cell, help encode motion direction (Yoshida et al, 2001). Ganglion cells, the retina's terminal output neuron, integrate these inputs across broad dendrites, and the balance of excitatory and inhibitory inputs determines whether an action potential, or spike, is fired. In the human retina, ~1 million ganglion cells, spanning ~18 different subtypes, generate diverse spike patterns that encode motion, contrast, color, luminance, and more, forming the neural code that instructs higher visual centers to construct a natural scene (Curcio and Allen, 1990; Kolb, Linberg & Fisher, 1992).

Normal visual development hinges on light-driven refinement of retinal circuits. But what happens when visual input is absent altogether? In cases of binocular deprivation, where a child is born blind in both eyes, visual maturation falters. Yet, the brain adapts. Deprived of vision, the child navigates the world using touch, hearing, and smell, each taking a greater role in shaping sensory pathways. Neuroplasticity drives this adaptation by reshaping the neural architecture to reflect the child's sensory reality. Psychophysical studies, which test sensory discrimination thresholds, confirm that people born blind have enhanced auditory and tactile perception compared to those with sight (Wan et al, 2010; Van Boven et al, 2000). This cross-modal example illustrates a core principle of

neuroplasticity: when one sensory input is lost, other inputs can be adjusted to compensate. The compensatory mechanism operates across all levels of neural organization, from entire sensory systems to individual circuits and cells.

Compensatory plasticity has long fascinated scientists and was central to the Nobel Prize winning work of Hubel and Wiesel. Their experiments revealed the existence of a critical period of sensory plasticity—a timeframe during which the visual cortex's potential for remodeling is greatest (Hubel and Wiesel, 1963). To understand its importance, consider monocular visual deprivation, where a child has one eye that functions normally while the other lacks visual input. This imbalance activates a competitive process governed by Hebbian plasticity; the principle famously quoted as "neurons that fire together, wire together", which leads to the functioning eye becoming dominant in terms of its cortical representation (Hebb, 1949).

Monocular deprivation triggers a cascade of synaptic remodeling in the visual cortex, where inputs from both eyes compete for dominance (Smith and Trachtenberg, 2007). The stronger input from the functioning eye undergoes a form of Hebbian plasticity called long-term potentiation (LTP). LTP operates via a feedback mechanism where increased activity reinforces stronger connections through expression of excitatory synapses that amplify signal transmission (Cooke and Bear, 2010). This is the same principle underlying memory formation in learning. In contrast, the deprived eye's inputs weaken its cortical connections through long-term depression (LTD), a complementary mechanism that selectively prunes underactive neural circuits, akin to the decay of forgotten learnings (Yoon et al, 2009). Over time, if visual input remains absent, LTD

similarly drives the decay of visual circuits, resulting in amblyopia—a condition where the visual cortex never ‘learns’ to see through the deprived eye.

However, if the cause of blindness is corrected within the critical period (typically before age 12), the brain retains enough plasticity to reorganize (Scheiman et al, 2005). Clinicians leverage this by covering the good eye with a patch, forcing the weaker eye to strengthen its cortical connections via reactivated LTP mechanisms. Yet, Hebbian plasticity alone cannot maintain stable visual circuits. If LTP and LTD operated without regulation, excessive potentiation could create runaway excitation loops, whereas unchecked depression could lead to irreversible synaptic atrophy (Abbott and Nelson, 2000). This is where homeostatic plasticity is recruited.

Unlike Hebbian plasticity, which strengthens or weakens individual synapses based on activity, homeostatic plasticity attempts to maintain the stability of neural networks (Vitureira and Goda, 2013). When input conditions change, homeostatic plasticity facilitates a new set-point that attempts to restore overall circuit function. While most active during development, homeostatic mechanisms persist into adulthood in two forms: cell-density-dependent and activity-dependent (Fitzpatrick and Kerschensteiner, 2023). These forms differ in their triggers and compensatory responses. Although large-scale visual circuit remodeling declines after the critical period, localized cellular plasticity continues throughout life.

The role of homeostatic plasticity becomes particularly evident in diseases of retinal degeneration such as retinitis pigmentosa (RP) that incrementally reduce afferent input in the network. RP, a genetic disorder, leads to progressive photoreceptor loss, triggering cell-density-dependent plasticity (Verbakel et al, 2018; Johnson et al, 2017).

Initially, the retina compensates for loss by maximizing the function of surviving photoreceptors. Even as photoreceptor outer segments degenerate, the inner segments continue transmitting light signals (Ellis et al, 2023). Meanwhile, downstream neurons including bipolar and ganglion cells undergo structural alterations such as dendritic remodeling and synaptic scaling that try to sustain synaptic efficacy as photoreceptor input declines.

Experiments in transgenic mice, where photoreceptor death is selectively induced via diphtheria toxin expression, reveal distinct strategies of synaptic plasticity. A 50% loss of rod photoreceptors prompts ganglion cells to reduce inhibitory receptors on their dendrites, matching the reduced excitatory input from bipolar cells (Care et al, 2020). Conversely, a 50% loss of cone photoreceptors leads de-partnered bipolar cells to sprout new dendrites, reconnecting with surviving cones (Care et al, 2019). Psychophysical studies in humans support these findings, showing that even with a 50% loss of cone photoreceptors, visual behavior remains largely normal (Ratnam et al, 2013; Seiple et al, 1995). These compensatory mechanisms prove remarkably effective in preserving vision during early to mid-stage degeneration. However, as photoreceptor loss progresses in late-stage RP, these mechanisms become overwhelmed. As circuit ensembles destabilize, disorganized activity emerges, leading to blindness and the vivid visual hallucinations of Charles Bonnet syndrome (O'Hare et al, 2015). This progression underscores the limits of neuroplasticity: compensatory responses can sustain function up to a point, beyond which alterations may become destabilizing.

Unlike RP, which disrupts multiple retinal pathways, models of complete congenital stationary night blindness (CSNB) lend insight into pathway-specific plasticity. CSNB is

neither degenerative nor progressive and selectively silences the ON retinal pathway, leaving the OFF pathway intact (Zeitz, Robson, & Aldo, 2015). This targeted suppression provides a compelling opportunity to study the limits of activity-dependent homeostatic plasticity and understand how input suppression shapes cellular- and circuit-level compensations underlying visual behavior. By using partial (~50%) or complete (100%) genetic knockout of the ON pathway function in mice, we can delineate adaptive and destabilizing mechanisms more clearly and reveal critical windows for therapeutic intervention.

This raises the fundamental question of this thesis: how much input suppression can retinal circuits endure before plasticity fails and function destabilizes? In Chapter 2, we will first explore how partial suppression of the ON pathway recruits adaptive mechanisms, such as increasing excitatory synapses in ON and OFF ganglion cell dendrites, to maintain signal transmission and visual behavior. Then, we will reveal the maladaptive consequences of complete ON pathway suppression, which destabilizes retinal circuits through intrinsic alterations of ganglion cells in both pathways, collectively rendering the animal blind. Traditional approaches like eye-patching therapy for amblyopia prevention illustrate how plasticity can be harnessed for functional recovery. However, treating diseases driven by gradual or sustained input suppression at the cellular level requires a more nuanced approach. The cases of RP and CSNB represent the limits of current clinical intervention. A deeper understanding of how cellular alterations shape structure and function over time is needed to enable timely and effective therapies.

One of the most promising technologies in this regard is adaptive optics scanning light ophthalmoscopy (AOSLO). AOSLO imaging offers a breakthrough by providing views of photoreceptor structure and function within the living human retina (Wynne, Carroll, Duncan, 2021). While current imaging techniques such as optical coherence tomography (OCT) provide valuable cross-sectional views of the retinal layers, it can miss subtle cellular alterations that impact vision (Kolli et al, 2023). AOSLO images show a more comprehensive landscape view of the photoreceptor mosaic across retinal regions. Its finer resolution is useful for monitoring conditions such as acquired retinal degeneration and inherited retinal dystrophies, which currently lack effective treatments. However, ongoing clinical trials for gene therapy and stem cell therapy offer hope to millions worldwide enduring the progressive decline of their visual experience.

A key challenge for such emerging therapies is determining when to intervene. If treatment is delayed too long, neuroplastic mechanisms may become overwhelmed, leading to entrenched maladaptive alterations that resist therapeutic correction. Consistent with this hypothesis, a recent study showed that delivering gene therapy to mouse models of retinitis pigmentosa restored retinal output function to wild-type levels with 25% and 50% loss of rod photoreceptors but resulted in continued deterioration of signal fidelity with 75% loss (Scalabrino et al., 2023). Therefore, having the ability to track structural and functional photoreceptor changes in real time is key for defining this critical inflection point in humans. AOSLO imaging has the potential to support clinical decision-making and is a tool capable of monitoring photoreceptor health and assessing therapeutic response. In Chapter 3, the closing discussion of this thesis, we will explore this potential further along with promising treatments like gene therapy. Ultimately, the

unifying theme of this thesis is that understanding visual neuroplasticity in health and disease is fundamental to preserving and restoring vision.

Building on the discussion of therapeutic windows, a key question that arises from these considerations is how much ON pathway suppression the retina can tolerate before compensation fails. Although mild disruptions often trigger homeostatic adjustments that help preserve functional output, advanced stages of retinal disease may surpass the circuit's adaptive capacity and lead to maladaptive reorganization. In the chapters that follow, I examine two distinct genetic models of ON pathway suppression, one with partial (~50%) mGluR6 reduction and another with a complete knockout of mGluR6, to explore the boundaries and mechanisms of retinal plasticity. Comparing these scenarios provides insight into why certain therapies remain effective in earlier stages of disease but may offer little benefit once a critical threshold of circuit disruption is crossed.

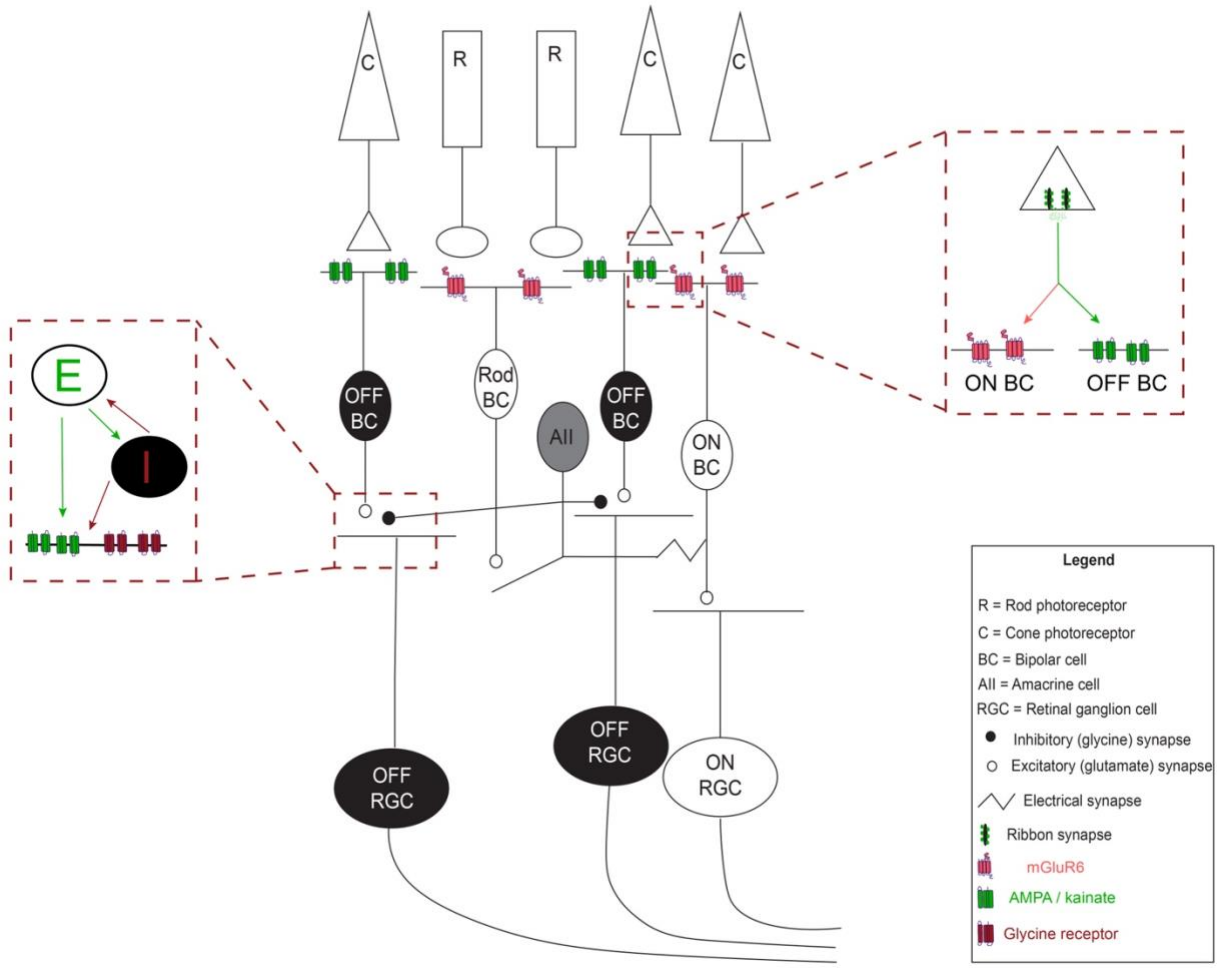

Figure 1. Simple schematic of synaptic layers in the mammalian retina.

In the outer plexiform layer (OPL), ON and OFF pathways diverge based on differential glutamate receptor expression: mGluR6 in ON bipolar cells dendrites versus AMPA/kainate in OFF bipolar cell dendrites. Both pathways receive glutamatergic input from photoreceptor ribbon synapses (*right box*). In the inner plexiform layer (IPL), bipolar cells (excitatory transmission, “E” in green) connect with ganglion cell dendrites that carry both excitatory (green) and inhibitory (red) postsynaptic receptors, while amacrine cells provide inhibitory, glycinergic input (“I” in red) to both bipolar cell terminals and ganglion cell dendrites. The AII amacrine cell, specifically, receives input from the ON pathway and delivers inhibition onto both bipolar cell axon terminals and ganglion cells in the OFF pathway, allowing crossover inhibition from ON circuits. This balance of excitatory and inhibitory signals ultimately determines whether a retinal ganglion cell fires an action potential.

Chapter 2: Mechanisms Underlying Neural Adaptation in the Mammalian Retina

This chapter has been submitted for publication.

Jacob Khoussine, Abhilash Sawant, Sapan Gupta, Pawan K. Shahi, Bikash R. Pattnaik, Raunak Sinha, Mrinalini Hoon

Introduction

The mammalian retina consists of neural circuit ensembles that act in concert to encode and transmit visual information from the eye to the brain. Our ability to see from starlight to daylight depends on the interplay between the ON and OFF retinal pathways (Wassle, 2004, Ala-Laurila and Rieke, 2014, Chichilnisky and Kalmar, 2002, Werblin and Dowling, 1969). Retinal neurons in the ON pathway depolarize to light increments, whereas retinal neurons in the OFF pathway depolarize to light decrements (Wassle, 2004). Although mostly segregated, there is crosstalk from the ON to the OFF pathway in the inner retina (Manookin et al, 2008, Schiller, 1982). Disruption of the ON input stream can therefore have significant consequences for signal transformation and output across both pathways, such as impairing luminance and contrast processing. Such visual processing impairments of the retina are observed in the disease complete congenital stationary night blindness (CSNB), where genetic suppression of the ON pathway causes individuals to experience night blindness with overall normal daylight vision. CSNB is a non-degenerative genetic condition characterized by a signaling imbalance between the ON and OFF pathways during retinal development (Zeitz et al., 2015). While previous studies have provided insights into the immediate functional consequences of ON pathway suppression through pharmacology (Murphy and Rieke, 2006, Manookin et al., 2008, Slaughter and Miller, 1981, Horton and Sherk, 1984, Zaghloul et al., 2003), the

mechanisms of neural compensation that can be engaged in response to chronic input suppression during circuit formation are not understood.

A deeper understanding of how the retina adapts - or fails to adapt - to chronic input suppression provides an opportunity to uncover the modalities of plasticity that retinal circuit elements and sensory circuit constituents can engage. Chiefly, this work is concerned with mechanisms of homeostatic plasticity, which are triggered in response to changes in cell density or synaptic activity. Earlier studies in transgenic mice showed that as photoreceptor density declines, cellular and synaptic components across cell types can restructure to attempt to maintain signal output fidelity. Indeed, visual circuits exhibit remarkable resilience to disruption, but more critically when is the tipping point at which plasticity mechanisms fail? When mouse models of photoreceptor degeneration are rescued with gene therapy, recovery in signal output to wild-type levels is achieved with 25% and 50% loss of rod photoreceptors but is unsuccessful beyond 50% loss (Scalabrino et al, 2023). There is thus a limit to how much cell death can occur before therapeutic correction is resisted. However, the activity-dependent homeostatic plasticity mechanisms recruited to counteract varying degrees of input suppression remain unknown. This study aims to fill this gap by defining the neural compensation mechanisms at the level of the output retinal ganglion cells (RGCs) in response to partial and complete ON pathway suppression in two genetic mouse models across dim- to bright-light luminance conditions.

To address this question, we used CRISPR-mediated gene editing to generate two models of suppressed ON pathway input. We targeted the *Grm6* gene, which encodes for a specific metabotropic glutamate receptor (mGluR6) that is localized on the dendrites

of ON retinal bipolar cells and receives photoreceptor input (Fig 1A). We focus on the consequences of partial (~50%) and complete (100%) elimination of mGluR6 in heterozygous (HET) and homozygous (KO) *Grm6* knockouts, respectively. By comparing these two models, we dissected how varying degrees of ON pathway suppression impact RGC output profiles and their capacity to engage compensatory mechanisms affecting retinal function across both the ON and OFF pathways.

Of note, ON and OFF retinal pathways are established at the very first synapse in the retina (Wassle, 2004, Hoon et al., 2014, Masland, 2001). This is primarily done through specific bipolar cells that use distinct receptors to respond differentially to the glutamate released by photoreceptors. Specifically, ON bipolar cells express the retina-specific metabotropic glutamate receptor mGluR6, whereas OFF bipolar cells express conventional ionotropic (AMPA/kainate) glutamate receptors (Nomura et al., 1994, Vardi et al., 2000, DeVries, 2000). Disruption of proteins involved in ON pathway signal transduction, such as mGluR6, leads to CSNB (Zeitz et al., 2015; Masu et al., 1995, Dryja et al., 1993, van Genderen et al., 2009, Peachey et al., 2012, Maddox et al., 2008, McCall and Gregg, 2008). Though ON and OFF bipolar cells synapse onto dedicated ON and OFF RGCs, there is crosstalk between the ON and OFF retinal pathways. Specifically, in the inner retina, the AII amacrine cell, a specialized interneuron activated by ON bipolar cells (Demb and Singer, 2012), provides robust glycinergic inhibition to the OFF bipolar (Manookin et al., 2008, Hoon et al., 2015) and ganglion cells (Grimes et al., 2022, Munch et al., 2009). This ‘crossover’ inhibition can tune the excitability of the OFF pathway RGCs (Grimes et al., 2022). Activation or suppression of the ON pathway thus also shapes the input and output profiles of the OFF pathway.

To clarify the structural and functional modifications that occur in response to these different degrees of input suppression, we combined single cell electrophysiology with immunohistochemical assays of synaptic protein expression levels. This approach allowed us to uncover differential modes of compensation recruited by RGCs in a cell-type and circuit-specific manner. In particular, we discovered that synaptic compensation is preferentially recruited when the ON pathway is partially suppressed. Conversely, alterations in the RGC intrinsic properties are invoked when the ON pathway is completely suppressed. We also discovered one OFF RGC pathway that is pushed into cyclical instability after complete input suppression. To determine whether the alterations in each genetic model conferred an adaptive or maladaptive compensatory response, we coupled our cellular and biophysical assays of retinal ganglion cell function with visual behavior assays for each model. Overall, our findings unveil new insights into retinal circuit adaptability and instability imposed by imbalanced sensory input.

Results

Elimination of mGluR6 Selectively Suppresses ON Pathway Excitation

Functional dichotomy within the retinal circuit is established by the expression of distinct glutamate receptors on the dendrites of ON and OFF bipolar cells - the second-order neurons receiving photoreceptor input. Depending on their operation range, there are two broad types of photoreceptors in the murine retina – rod photoreceptors that operate at dim-light conditions and cone photoreceptors that respond in bright light conditions (Lamb, 2016). Each photoreceptor sends information to type-specific rod and cone bipolar cells. Rod bipolar cells are of the ON type, but cone bipolar cells can be of

both ON and OFF types. In addition to establishing glutamatergic synapses with bipolar cell dendrites, rod and cone photoreceptors also establish electrical gap junctional connections amongst themselves (Jin et al., 2020). **Figure 1A** illustrates how rod and ON cone bipolar cells (such as the Type 6 or T6) expressing mGluR6 transmit signals to AII amacrine cells via glutamatergic and electrical synapses. These inputs drive glycinergic crossover inhibition of OFF bipolar cells (such as T2 or T3) and OFF ganglion cells (Manookin et al., 2008, Marco et al., 2013, Rosa et al., 2016). In tandem, ON and OFF cone bipolar cells relay excitatory input to their respective alpha RGC subtypes – ON and OFF RGCs - each generating distinct action potential spiking (spike output) patterns to the LGN (Krieger et al., 2017, Pang et al., 2003).

Alpha RGCs comprise major retinal ganglion cell output pathways in the mouse retina and are characterized by large, mono-stratified dendritic arbors and large soma sizes (Murphy and Rieke, 2006, Krieger et al., 2017, Pang et al., 2003). Each of these alpha RGC types also have a characteristic response profile and ON and OFF RGCs can be further subdivided depending on the duration of their response. ON sustained RGCs demonstrate a sustained elevation in spike output during light increments. OFF sustained RGCs show a sustained elevation in spiking during light decrements (Fig 1A). Whereas OFF transient RGCs exhibit a transient burst in spiking upon light decrements or at the offset of a light increment (Krieger et al., 2017). Our study focused on ascertaining the response profiles and synaptic protein distribution of these three alpha RGC types in the two mouse models where ON pathway input was selectively and differentially suppressed.

To disrupt ON pathway excitation, we used CRISPR gene editing to generate transgenics that eliminate the metabotropic glutamate receptor mGluR6, which is crucial for transmitting signals from photoreceptors to ON bipolar cells and is a receptor whose dysfunction is related to CSNB. We generated two mouse models to investigate neural circuit alterations associated with CSNB: a heterozygous model with a 50% reduction of mGluR6 expression (HET) and a knockout model with complete elimination (KO). In these CSNB models, excitatory input from photoreceptors to rod and ON cone bipolar cells is selectively suppressed, keeping the OFF pathway intact. We confirmed that our *Grm6* KO leads to no mGluR6 expression at bipolar cell dendrites by performing whole-cell recordings from rod bipolar cells in a slice preparation and assessing the response to a puff of the mGluR6 antagonist, CPPG (cyclopropyl-4-phosphonophenylglycine), applied at the dendrites (Nawy, 2004, Morgans et al., 2009). Rod bipolar cells were first bathed in L-AP4 (20 mM; mGluR6 agonist) to mimic darkness followed by a dendritic puff of CPPG (500 mM) to simulate a light flash. Wildtype (WT) control rod bipolar cells show a clear response to CPPG (Fig S1A), HET rod bipolar cells show close to 50% response, and KO rod bipolar cells lack this response (quantification of response amplitude across genotypes in Fig S1A'). As another level of confirmation, we performed electroretinogram (ERG) recordings in the rod-dominated (scotopic) light regime from the *Grm6* KO mice and observed no b-wave response (Fig S1B). ERGs in this regime typically consist of an a-wave component reflective of the efficiency of phototransduction, and a b-wave component representing the rod→rod bipolar cell activation (Stockton and Slaughter, 1989, Robson and Frishman, 2014). This b-wave is reliant on the presence of mGluR6 at bipolar cell dendrites. The lack of the b-wave in our KOs confirms the absence of mGluR6

expression. Of note, the lack of the ERG b-wave is also characteristic of the CSNB model phenotype (Zeitz et al., 2015).

Partial and Complete Input Suppression Invoke Divergent Plasticity Mechanisms

We next focused on the ON sustained alpha RGC because it is the major ON retinal output pathway in the mouse retina, and we wanted to understand how response profiles compared between partial and complete input suppression. We performed cell-attached and voltage-clamp electrophysiology from the ON sustained alpha RGCs across HET and KO genotypes to record spike output and synaptic inputs, respectively, in response to a dim 10 R*/rod/sec light flash from darkness (Fig 1B). In HET ON sustained RGCs, both excitatory and inhibitory synaptic inputs and spike output remained intact and comparable to WT RGCs, suggesting that partial loss of mGluR6 may trigger a compensatory response that preserves ON pathway function. In contrast, KO RGCs lacking mGluR6 entirely displayed no light-evoked responses, confirming complete suppression of the ON pathway (Fig 1B). Our voltage-clamp recordings further confirmed the lack of both light-driven excitation and inhibition in the KO ON sustained alpha RGCs (see FigS2 for exemplar traces). These observations demonstrate that ~50% ON pathway suppression in the HET does not reduce ON signal transmission, whereas complete suppression in the KO abolishes it.

To determine whether suppression of the ON pathway elicits alterations in the intrinsic properties of ON sustained RGCs, we performed current-clamp recordings to measure the resting membrane potential of KO and HET ON sustained RGCs as compared to WT (Fig 2A). Interestingly, KO ON sustained RGCs were significantly

hyperpolarized compared to both WT and HET cells. This hyperpolarization may be due to a lack of tonic glutamate drive from the ON bipolar cell terminals in the KO throughout retinal development. Of note, the other intrinsic property parameters such as input resistance and capacitance remained unchanged in the KO RGCs (Fig 2A). To assess the functional consequences of the hyperpolarization in KO ON sustained RGCs, we performed current injections into ON sustained RGCs across genotypes (Fig 2B). With increasingly depolarizing currents, we observed that although KO ON sustained RGCs could generate spikes, they had a reduced spiking capacity compared to WT RGCs, which was consistent with the altered resting membrane potential of the KO RGCs. Together, these observations reveal that KO ON sustained RGCs have reduced excitability, suggesting that the cells may effectively enter a dormant state with reduced spontaneous activity in response to the prolonged, complete suppression of ON pathway activation.

We next investigated whether suppression of the ON pathway could lead to alterations in RGC synaptic protein levels. We filled individual ON sustained RGCs with neurobiotin via patch-clamp technique to facilitate immunohistochemical analyses of synaptic proteins across individual RGC dendrites (Fig 2C). Using antibodies against PSD95 to label excitatory glutamatergic postsynapses across RGC dendrites (Bleckert et al., 2013, Morgan et al., 2008) and GlyRa1 to label inhibitory glycinergic postsynapses (GlyRa1 being the predominant glycine receptor type in ON sustained RGCs (Majumdar et al., 2007)), we assayed the expression of these synaptic proteins within the dendrites of ON sustained RGCs across genotypes (Fig 2C). We masked the dendritic volume of each ON sustained RGC and quantified the density of PSD95 and GlyRa1 expression by

calculating the percentage volume occupancy of each receptor type relative to the masked dendritic volume (Hoon et al., 2017; see *Methods* for details).

Remarkably, we found that HET ON sustained RGCs showed a significant upregulation of excitatory synaptic proteins as assayed by the percent occupancy of PSD95 within the dendritic arbor, whereas KO ON sustained RGCs had expression levels of the synaptic proteins that were comparable to WT (Fig 2C). This suggests that the upregulation of excitatory synapses in HET ON sustained RGCs could compensate for the partial reduction in upstream excitatory drive, explaining why voltage-clamp recordings in HET ON sustained RGCs showed no difference in peak excitatory currents compared to WT. These experiments reveal that the two models recruit different compensatory mechanisms: HET ON sustained RGCs increase expression of excitatory synaptic proteins, whereas KO ON sustained RGCs reduce their excitability, underscoring that the extent of perturbation determines the compensatory responses recruited.

Reduced ON Pathway Activity Impairs OFF Pathway Spike Output and Contrast Encoding

Given our observations for the ON pathway output in the two models, and the well-established mechanism of crossover inhibition from the ON to the OFF pathway (Manookin et al., 2008, Munch et al., 2009), we sought to understand how OFF RGCs cope with imbalanced synaptic input when the ON pathway is chronically suppressed. We first focused on the OFF sustained alpha RGC. Under normal conditions, the OFF sustained RGC spikes constantly in darkness, suppresses spiking during light stimulation, and exhibits increased spiking following light offset (Fig 3A). We recorded spike output

across three different luminance levels (10 R*/rod/sec, 1000 R*/cone/sec and 5000 R*/cone/sec) in OFF sustained RGCs for each genotype and quantified baseline spiking, duration of spike suppression during light stimulation, and peak spike rate following light offset (Fig 3A-B). 10 R* light levels represent rod-driven scotopic signaling, 5000 R* represent cone-driven photopic conditions and 1000 R* represents intermediate (mesopic) light conditions.

We discovered a luminance-dependent dysfunction in both HET and KO OFF sustained RGCs. In HET cells, deficits were primarily observed at the lower luminance levels. Specifically, baseline spiking was elevated at 10 R*/rod/sec, and both the spike suppression duration and peak spike rate were reduced in HET OFF sustained RGC compared to control (Fig 3B top panel). In KO OFF sustained RGCs, the deficits in the spike suppression and peak spike rate at light offset were much more pronounced, especially the ability of the KO OFF sustained RGCs to suppress spikes during a light flash, which was severely impaired at lower light levels (Fig 3A-B). From darkness, we applied a 10 R*/rod/sec light flash and KO OFF sustained RGCs were completely unable to suppress spikes during light stimulation. Interestingly, as luminance increased, cellular function improved in both the HET and KO models. At 1000 R*/cone/sec, HET OFF sustained RGCs were not significantly different from WT in baseline spiking and spike suppression duration. KO cells showed some improvement in spike suppression compared to the deficits seen with 10 R*/rod/sec. By 5000 R*/cone/sec, OFF sustained RGCs in both HET and KO models could suppress spikes normally, but KO cells continued to exhibit elevated baseline spiking. They also showed a significant reduction in the peak spike rate at light offset (Fig 3B bottom panel). Together, these observations

highlight an impairment in the ability of the OFF sustained RGCs to encode for luminance variations when the ON pathway input is suppressed. This deficit is particularly pronounced at the dim-light regime.

A primary function of the OFF sustained RGC in the murine retina is contrast encoding; it is among the most contrast-sensitive RGCs (Marco et al., 2013). Based on the above deficits to light stimuli, we hypothesized that the spike output deficits of the OFF sustained RGCs in the CSNB models would exhibit in a reduction of contrast sensitivity. To test this, we applied background luminance of 1000 R* or 5000 R*/cone/sec to adapt the retinal circuits and then presented 500ms light flashes with incremental intensity changes above and below the background to establish contrast response curves for the OFF sustained RGCs across genotypes (Fig 3C). In WT and HET OFF sustained RGCs, the contrast response curves displayed the expected sigmoidal shape consistent with previous literature (Marco et al., 2013). However, KO OFF sustained RGCs were almost insensitive to contrast at both background luminance levels and incapable of encoding contrasts (Fig 3C). The slope of the contrast response curve (inset Fig 3C) was significantly reduced for KO OFF sustained RGCs at both 1000 R* and 5000 R*/cone/sec light levels. For HET OFF sustained RGCs, the slope was significantly reduced compared to control only at the bright light level (5000 R*/cone/sec, bottom inset Fig 3C). These deficits in contrast sensitivity observed at the level of retinal output were also recapitulated in visual behavior responses as determined through the optomotor response assay (Fig S3). We conducted this assay under both dim-light and bright-light conditions to isolate contributions of rod- and cone-mediated circuits. We measured visual behavior in response to contrast gratings and spatial stimuli (protocol similar to Prusky et al., 2004).

These experiments showed decreased visual acuity and contrast sensitivity of KO animals, whereas WT and HET animals had comparable responses. These observations imply that the aberrancies in retinal output observed in the KO animals also lead to visual behavior issues, specifically in terms of deficits in visual acuity and contrast sensitivity.

To understand the drivers of the spike output deficits observed in the mutant OFF sustained RGCs, we recorded peak excitatory and inhibitory synaptic currents from OFF sustained RGCs across luminance levels and genotypes (Fig 4A). Of note, the excitatory input to OFF sustained RGCs is primarily through OFF bipolar cells, whereas the crossover inhibitory input to these cells from the ON pathway is primarily through the AII amacrine cell (Grimes et al., 2022). In keeping with the lack of ON pathway input, the inhibitory current to KO OFF sustained RGCs during the incremental light flash was abolished entirely at all luminance levels (Fig 4A-B) due to the absence of crossover inhibition from the ON pathway (Manookin et al., 2008, Pang et al., 2007). Surprisingly, the excitatory current at light offset was also significantly reduced for the KO OFF sustained RGCs at all luminance levels except 5000 R*/cone/sec (Fig 4B). The reason that excitation was relatively normal at 5000 R*/cone/sec could be because at this background luminance level there is a saturation of the rod pathway and thus a reduced reliance on the AII-mediated disinhibition of the OFF pathway (Manookin et al., 2008, Pang et al., 2007). Together our observations from these voltage-clamp experiments underscore alterations in the synaptic input profiles of OFF sustained RGCs across the two CSNB models in a light-level and genotype-specific manner.

To understand the synaptic physiology underlying the contrast encoding deficits of OFF sustained RGCs, we next generated excitatory and inhibitory contrast response plots

for the OFF sustained RGCs at 5000 R*/cone/sec. The excitatory response curve revealed that KO OFF sustained RGCs had impairments in distinguishing deviations in negative contrast (Fig 4C). The slope of the excitatory contrast response curves was also significantly reduced for the KO RGCs compared to controls (Fig 4C) highlighting reduced sensitivity of the KO OFF sustained RGCs. It is well-established that the ON pathway rectifies the OFF pathway via inhibition, which shapes OFF pathway excitation non-linearly to enable complex encoding functions such as contrast sensitivity (Liang and Freed, 2010). The rectification index for an RGC scales from -1 (negatively rectified) to +1 (positively rectified); a negatively rectified RGC has larger responses to negative contrasts (-50%) than to positive contrasts (+50%) (Grimes et al., 2014). Normally, the OFF sustained RGC should be negatively rectified, which we find in our WT OFF sustained RGCs. Although not significantly different from the control, the KO OFF sustained RGCs had a rectification index trending towards zero at 5000 R*/cone/sec (Fig 4C), indicating a reduced preference for negative or positive contrasts. The lack of ON pathway inhibition could thus be responsible for the impaired contrast sensitivity of the KO OFF sustained RGCs.

HET and KO OFF Sustained RGCs Also Display Divergent Compensatory Responses

The partially impaired response profiles of HET OFF sustained RGCs, and the severely impaired profiles of KO RGCs, led us to hypothesize that alterations in intrinsic properties and synaptic protein expression might be informative to understand the underlying potential compensatory mechanisms being engaged by the OFF pathway. To this end, we first performed immunolabeling for the excitatory and inhibitory postsynaptic

proteins across the dendrites of OFF sustained RGCs by filling the RGCs with neurobiotin and performing co-labeling for PSD95 and GlyRa1 (Fig 5A). PSD95 labels the excitatory postsynapses across OFF sustained RGCs (Morgan et al., 2008, Bleckert et al., 2013) and GlyRa1-positive synaptic clusters are abundantly present across OFF sustained RGC dendrites (Sawant et al., 2021). HET OFF sustained RGCs exhibited increased PSD95 expression compared to control with a trend towards reduced expression of GlyRa1 compared to control RGCs (Fig 5A). Although glycine is the predominant inhibitory neurotransmitter for OFF sustained RGCs (Manookin et al., 2008, Marco et al., 2013), we did not observe significant alterations in the GlyRa1 expression across the HET and KO RGCs as compared to control. This was unexpected because the 50% reduction in mGluR6 expression *should* reduce excitatory drive through the ON pathway, decreasing input to AII amacrine cells and thus reducing inhibitory input to OFF sustained RGCs. The finding that PSD95 expression is upregulated but not GlyRa1 in OFF RGCs suggests that 1) optimization of excitation is critical for neural function and 2) perhaps other intermediary neurons in the circuit have alterations that contribute to our findings.

In contrast, the KO OFF sustained RGCs did not show significant alterations in synaptic protein expression levels compared to control. The KO OFF sustained RGCs did however undergo alterations in their intrinsic properties as measured by current clamp recordings of these cells across genotypes. The KO OFF sustained RGCs became significantly more depolarized and excitable compared to HET and WT OFF sustained RGCs while maintaining normal input resistance (Fig 5B). The KO cells also went into depolarization-block more frequently (Fig 5B lower panel) underscoring the enhanced intrinsic excitability of the OFF sustained RGCs. Thus, consistent with the divergent

compensatory mechanisms observed in mutant ON sustained RGCs, OFF sustained RGCs also engage in synaptic or intrinsic mechanisms of compensation to address input imbalance across the two models.

Different OFF Circuits Have Distinct Consequences of Imbalanced Synaptic Input

Next, we investigated the response profiles of another major OFF output type - the OFF transient RGC (Munch et al., 2009). Strikingly, even though the OFF transient RGCs are subject to the same input manipulation as the OFF sustained RGCs in the CSNB models, their response to the ON pathway input blockade in the KO led to severe spike output aberrations. OFF transient RGCs have a relatively low baseline spike rate and typically generate a transient burst of spikes upon light offset. This pattern was observed for both WT and HET OFF transient RGCs across luminance levels (Fig 6A). For KO OFF transient RGCs, however, we observed an aberrant spike burst behavior that was most prominent at low luminance levels, but which persisted across all luminance levels (Fig 6). As luminance increases, the presence of the expected transient burst at light offset became more apparent for the KO OFF transient RGCs (Fig 6). Thus, similar to the KO OFF sustained RGCs, the KO OFF transient RGCs also display less aberrant response profiles at bright-light levels. Nonetheless, the aberrant bursting pattern of the KO OFF transient RGCs prevents normal information encoding as demonstrated by the quantifications of the peak spike rate at light offset and the number of spikes during the light step (Fig 6B). The peak spike rate at light offset was significantly reduced for the KO OFF transient RGCs at both the 10R*/rod/sec and 1000R*/cone/sec light levels. The failure of the KO OFF transient RGCs to suppress spikes during the light step was evident in the significant increase in the number of spikes during the light stimuli for the

10R*/rod/sec and 5000R*/cone/sec light levels (Fig 6B). Next, we examined the excitatory and inhibitory synaptic drivers of the KO OFF transient RGC spike burst aberrancy.

To this end, we first performed voltage-clamp recordings from OFF transient RGCs across genotypes and compared the excitatory and inhibitory currents across the three luminance levels (Fig 6C). Similar to the OFF sustained RGCs, KO OFF transient RGCs receive little to no inhibitory input across luminance levels. Excitatory currents of KO OFF transient RGCs are reduced at low and moderate luminance compared to WT and HET cells but were normal at high luminance. The HET OFF transient RGCs had elevated excitation in response to 10 R*/rod/sec flashes but showed reduced excitation and inhibition at 1000R*/cone/sec luminance level compared to control (Fig 6C-D).

Interestingly, analysis of the excitatory and inhibitory waveforms in KO OFF transient RGCs also revealed oscillatory, burst-like behavior. We measured the frequency of the excitatory, inhibitory, and spike burst events from the KO OFF transient RGCs and observed that each occurs at a common frequency of approximately 3 Hz (Fig 6E). This frequency is significantly different from the oscillatory bursts observed in models of retinal degeneration, suggesting a distinct mechanism for generation of these oscillatory activity profiles in the KO CSNB model (see Discussion for details). Since we have removed ON pathway-mediated inhibitory input to the OFF transient RGCs in the KO CSNB model, the inhibitory oscillations may be a response to feedforward excitation bursts from the OFF bipolar cell. Alternatively, we hypothesized that a shift in the resting membrane potential of the KO OFF transient RGC to a more excitable, depolarized state could result in spike bursts. To test this, we performed current-clamp recordings from KO OFF transient RGCs and compared their resting membrane potential to control RGCs. We found no evidence

of a shift in KO OFF transient RGC resting membrane potential compared to WT (Fig 6F). However, current injections into KO OFF transient RGCs elicited a remarkably higher spike output compared to WT cells, suggesting enhanced intrinsic excitability of KO OFF transient RGCs. This could suggest perturbed active properties of KO OFF transient RGCs probably due to altered ion channel expression. Taken together, our observations revealed aberrant activity profiles and enhanced excitability of OFF transient RGCs when ON pathway input is completely suppressed.

Pharmacologic Blockade of the ON Pathway Clarifies Impact of Transient vs. Chronic Suppression

A critical aspect of this study is understanding the compensatory mechanisms that occur in retinal output pathways due to chronic perturbation of ON pathway input in the retina. To distinguish between the impact of chronic suppression in our KO model and alterations that could emerge from a transient suppression of ON pathway input, we next compared the KO OFF sustained RGC spike responses with those of WT RGCs subject to a pharmacological suppression of ON pathway input. We used the mGluR6 agonist APB in WT retinas to suppress ON pathway function transiently (Slaughter and Miller, 1981). After confirming suppression of light-evoked spike output from ON sustained RGCs and crossover inhibitory input to OFF RGCs, we recorded the spike output of OFF sustained and transient RGCs across luminance levels and compared the responses in APB retinas with those from KO mice (Fig 7A).

Interestingly, the extent of spike suppression during the light flash, and the improvement in spike suppression as luminance increased were similar in both the

pharmacologic (APB-treated) and KO conditions. The APB condition also reduced peak spike output similar to the KO, which improved as luminance increased to 5000 R*/cone/sec. However, only the KO condition exhibited persistent elevations in baseline spiking across luminance levels providing a clue that this effect was likely due to the chronic input suppression (Fig 7B). Of note, our observation that KO OFF sustained RGCs have a more depolarized resting membrane potential likely accounts for the elevated baseline spiking activity of the KO OFF sustained RGCs. Since changes in resting membrane potential may take longer to manifest as seen in the KO, the OFF sustained RGCs subject to a pharmacologic blockade of ON pathway input by APB would not be expected to alter excitability via shifting the neuron's resting membrane potential.

Finally, we determined the contrast encoding capability of the APB-treated OFF sustained RGCs compared to KO OFF sustained RGCs (Fig 7C). At 1000R*/cone/sec the APB treated OFF sustained RGCs did not demonstrate deficits in contrast encoding whereas the KO OFF sustained RGCs showed significant deficits (Fig 7C top panel). At 5000 R*/cone/sec the APB treated OFF sustained RGCs showed some deficits for encoding negative contrasts, but this impairment was not as dramatic as the KO OFF sustained RGCs (Fig 7C bottom panel). Together, our findings reveal that the elevated baseline spiking and intrinsic excitability of the KO cells disrupts their ability to encode contrast effectively at intermediate and bright-light conditions. This further emphasizes that the intrinsic property alterations in the KO are maladaptive compensations that do not promote complex OFF RGC function.

Methods

Retinal Preparations

Slice Preparation: All procedures conformed to institutional guidelines and were approved by the Institutional Animal Care and Use Committee (IACUC). Mice were euthanized by cervical dislocation, and eyes were immediately enucleated. Retinas were dissected from the eyecup into small trapezoidal pieces in warm Ames medium (Sigma-Aldrich), continuously bubbled with 95% O_2 and 5% CO_2. The retinal pieces were embedded in low-melting-point agarose and sectioned at about 200 µm thickness using a Leica vibratome. Sections were then transferred to the recording chamber and visualized under 60X magnification for targeting cells of interest for single cell electrophysiology.

Whole-Mount Preparation: Under infrared illumination, retinas were dissected from the eyecup in darkness. The temporal retina was isolated, specifically the ventral temporal region, and the vitreous was carefully removed. The tissue was flat-mounted on poly-D-lysine–coated glass coverslips and secured with a custom-made harp grid. The preparation was transferred to a recording chamber and super-fused with oxygenated (95%O_2 / 5% CO_2) Ames medium (Sigma-Aldrich) at 31°C–33°C at a rate of ~6 mL/min. The tissue was allowed to equilibrate for 10 minutes before recordings.

Electrophysiology

Slice recording: Retinal slices were placed in a recording chamber perfused with oxygenated Ames medium at 31°C–33°C with a flowrate of ~6 mL/min. Rod bipolar cells were identified according to their stereotypic morphological features (Sinha et al., 2021, Sinha et al., 2020). Whole-cell patch-clamp recordings were performed using borosilicate

glass pipettes with a resistance of 8–10 MΩ. Pipettes were filled with an intracellular solution containing (in mM): 105 Cs methanesulfonate, 10 TEACl, 20 HEPES, 10 EGTA, 2 QX-314, 5 Mg-ATP, 0.5 Tris-GTP (~280 mOsm; pH ~7.3 with CsOH). To quantify mGluR6 expression, puff applications of mGluR6 antagonist, α-cyclopropyl-4-phosphonophenylglycine (CPPG), were performed. 0.1mM Alexa-488 hydrazide was used for visualization of the CPPG puff. CPPG was applied at the dendrites of the rod bipolar cells in the outer plexiform (synaptic) later of the retina via pressure ejection using a Picospritzer II (General Valve) for a duration of 50ms. The puff location was confirmed by the fluorescence of Alexa 488. Rod bipolar cells were voltage-clamped at approximately -60mV and were bathed in L-AP4 (20 mM; mGluR6 agonist) to mimic darkness followed by a dendritic puff of the mGluR6 antagonist CPPG (500 mM) to simulate a light flash (Nawy, 2004, Morgans et al., 2009). Peak amplitudes of CPPG-evoked currents were measured by calculating the difference between the pre-stimulus baseline current and the peak response, averaged across multiple trials.

Whole-mount recording: Retinal ganglion cells (RGCs) were targeted using IR-DIC optics in a whole-mount retina preparation. ON and OFF alpha RGCs were identified based on their large soma size (≥ 20 µm diameter) and characteristic light response profiles. Of note, in the KO the ON sustained RGCs exhibited no response to light flash (see Fig 1 and Fig S2). After tearing a hole in the inner limiting membrane, cell-attached recordings were performed using pipettes with resistances of 3–5 MΩ filled with Ames media. Spike activity was recorded in response to full-field light stimuli (~450 µm diameter) delivered through the microscope condenser using a calibrated LED light source. Stimulus

intensities were set to 10 R*/rod/sec (green LED) and 1000 and 5000 R*/S-cone/sec (UV-blue LED).

Contrast Response Function Testing: RGCs were adapted to background illumination levels of either 1000 or 5000 R*/S-cone/s for at least 3 minutes to ensure steady-state adaptation. Contrast stimuli consisted of 500ms light increments and decrements relative to the background, with contrasts of –100%, –50%, –25%, +25%, +50%, +100%, and +200%. Spike counts were calculated by counting the number of spikes during the stimulus period and subtracting the baseline spike count obtained during an equivalent pre-stimulus period. Contrast response curves were generated by plotting the average change in spike count against stimulus contrast. The slope of the contrast response was determined for each cell over the contrast range from –50% to +25%, where the response was most linear. Voltage-clamp recordings were performed following the same protocol to isolate excitatory synaptic responses to contrast stimuli. From these excitatory contrast data, the rectification index was calculated as described in Grimes et al. 2014.

Voltage-Clamp Recordings: Whole-cell voltage-clamp recordings were sampled at 50 kHz and low pass filtered at 3 kHz. All electrophysiology data were acquired by a MATLAB-based data acquisition software (Symphony-DAS). Voltage-clamp recordings were obtained using pipettes filled with an intracellular solution containing (in mM) the following: 105 Cs methanesulfonate, 10 TEACl, 20 HEPES, 10 EGTA, 2 QX-314, 5 Mg-ATP, 0.5 Tris-GTP (~280 mOsm; pH ~7.3 with CsOH). To isolate excitatory postsynaptic currents (EPSCs), cells were held at the chloride reversal potential (approximately –60 mV). Inhibitory postsynaptic currents (IPSCs) were isolated by holding cells at the cation reversal potential (approximately 0 mV).

Current-Clamp Recordings: Whole-cell current-clamp recordings were performed on ON and OFF RGCs using a K-aspartate–based internal solution containing (in mM): 125 K-D/L aspartate, 1 MgCl2, 10 KCl, 10 HEPES (free acid), 2 EGTA, 1 CaCl2, 4 Mg-ATP, 0.5 Tris-GTP. Resting membrane potential was measured immediately upon establishing whole-cell configuration in darkness and averaged over multiple trials. Input resistance was calculated from the voltage response to hyperpolarizing current steps (–50 pA, 500ms duration) as per Ohm's law. Membrane capacitance was calculated using the equation C = t/R, where t is the membrane time constant, obtained from the exponential fit of the voltage response to hyperpolarizing current injection in Igor Pro 9, and R is the input resistance. Action potential firing was elicited by injecting depolarizing current steps ranging from 25 to 200 pA in 25 pA increments. Spike counts were quantified by counting the number of action potentials during each current step, averaged over multiple trials.

To suppress the ON pathway pharmacologically, 5 µM of 2-amino-4-phosphonobutyric acid (APB) was added to the perfusion solution. After 5 minutes of perfusion, suppression of the ON pathway was confirmed by the absence of light-evoked spiking in ON-sustained RGCs, and the elimination of inhibitory synaptic currents in OFF RGCs. Cell-attached recordings were then performed on OFF-sustained in response to stimuli at 10 R*/rod/sec, 1000 R*/S-cone/sec, and 5000 R*/S-cone/sec.

Electroretinogram (ERG) recordings

Animals were dark-adapted overnight and anesthetized with intraperitoneal injections of ketamine (80mg/kg) and Xylazine (16mg/kg). A drop of 0.5% proparacaine hydrochloride was applied to the eye for local anesthesia and a drop of 1% tropicamide was applied to

dilate the pupil. The mouse was kept on the heating pad at 37ºC to maintain the body temperature. Full-field ERG was performed using Espion system (Diagnosys LLC, MA) as reported previously (Jiao et al., 2021). All procedures were conducted under dim red light to maintain scotopic conditions. A recording electrode was placed on the corneal surface of the eyes which has a drop of sterile 2.5% hypromellose ophthalmic solution (Goniovisc, HUB pharmaceuticals LLC, CA). A reference electrode was inserted subcutaneously in the cheek, with a ground electrode in the base of the tail. Scotopic ERGs were recorded in response to flashes of light of varying intensities (0.1-10 Cd.s/m2), and the amplitudes of the a-wave and b-wave were quantified by measuring the baseline to the peak of each wave component (Jiao et al., 2021).

Optomotor Response (OMR) Assay

Visual acuity and contrast sensitivity were assessed under dim and bright conditions using an optomotor response (OMR) assay (OptoMotry, CerebralMechanics). Dark-adapted mice were placed on a platform at the center of four computer monitors displaying vertical sine wave gratings rotating at 12°/sec. Spatial frequency and contrast of the gratings were varied systematically. The OMR index was calculated as the ratio of head-tracking movements to stimulus presentations; an index above 1.1 was considered indicative of visual perception (Kretschmer et al., 2015). For visual acuity measurements, contrast was held constant at 0.8, where mice across genotypes had the best visual performance for the respective genotype, while spatial frequency was varied.

Immunohistochemistry

ON and OFF alpha RGCs were identified and patched in whole-cell configuration using pipettes filled with cesium-based internal solution containing neurobiotin (0.5%) as detailed in Sawant et al. 2021. Neurobiotin was allowed to diffuse into the cells for ~3 minutes. The retina was then removed from the recording chamber and fixed in 4% paraformaldehyde for 15 minutes at room temperature. After fixation, the tissue was rinsed in 0.1M phosphate-buffered saline (PBS) for 3 X 10 minutes. Thereafter the tissue was incubated with primary antibodies against PSD95 (rabbit, Synaptic systems) and GlyRa1 (mouse, Synaptic systems) on a shaker at 4°C for ~5 days in a blocking solution containing 5% donkey serum and 0.5% triton X-100. Following primary antibody incubation, the retina was rinsed in PBS 3 X10 minutes. Secondary antibodies were applied in PBS and incubated overnight at 4°C. Secondary antibodies included donkey anti-mouse Alexa Fluor 647 and donkey anti-rabbit Alexa Fluor 488 conjugate. Streptavidin conjugated to Alexa Fluor 568 was used to fluorescently label neurobiotin-filled RGCs. After rinsing in PBS (3 X 10 minutes), the retina was mounted onto a nitrocellulose membrane (Millipore HABG01300) and cover slipped on a glass slide. Vectashield (Vector labs) mounting medium was used.

Confocal Imaging and Quantification

Confocal z-stack images were acquired using a Leica SP8 confocal microscope equipped with a 63X oil immersion objective (NA 1.4). Images were captured with a voxel size of approximately 0.09 × 0.09 × 0.3 µm (x–y–z). Z-stacks were processed using ImageJ (NIH) for initial visualization and file transformation. Further analysis was performed using Amira

software (ThermoFisher Scientific). In Amira, individual RGC dendrites were isolated using the 'LabelField' function. Synaptic protein signals specifically within RGC dendrites were visualized using the Amira 'Arithmetic' function between the synaptic channel and the masked dendrites. Thereafter thresholding was applied for the synaptic channel to eliminate background noise. A threshold of three standard deviations above the background noise peak was typically used (for further details on threshold selection and analyses, see Hoon et al. 2017). The volume of detected pixels from the synaptic channel and the volume of RGC dendrites were calculated using custom MATLAB scripts (MathWorks, see Hoon et al. 2017). The volume occupancy of the synaptic marker relative to RGC dendrites was thereafter determined by calculating the percentage of the volume of the synaptic marker compared to the total RGC dendritic volume.

Quantification and Statistical Analysis

Statistical details including number of cells (n) and number of animals (N) are provided in the Figures or Figure Legends. All data is presented as mean ± SEM (standard error of mean). A two-tailed unpaired T-test was used to determine significance. $*$ $p<0.05$, $**p<0.01$ and $***$ $p< 0.001$. Blue asterisks in the Figures denote comparison between WT and HET; red asterisks in the Figures denote comparison between WT and KO; purple asterisks in the Figures denote comparison between HET and KO; green asterisks denote comparison between WT and APB-treated condition.

Figures

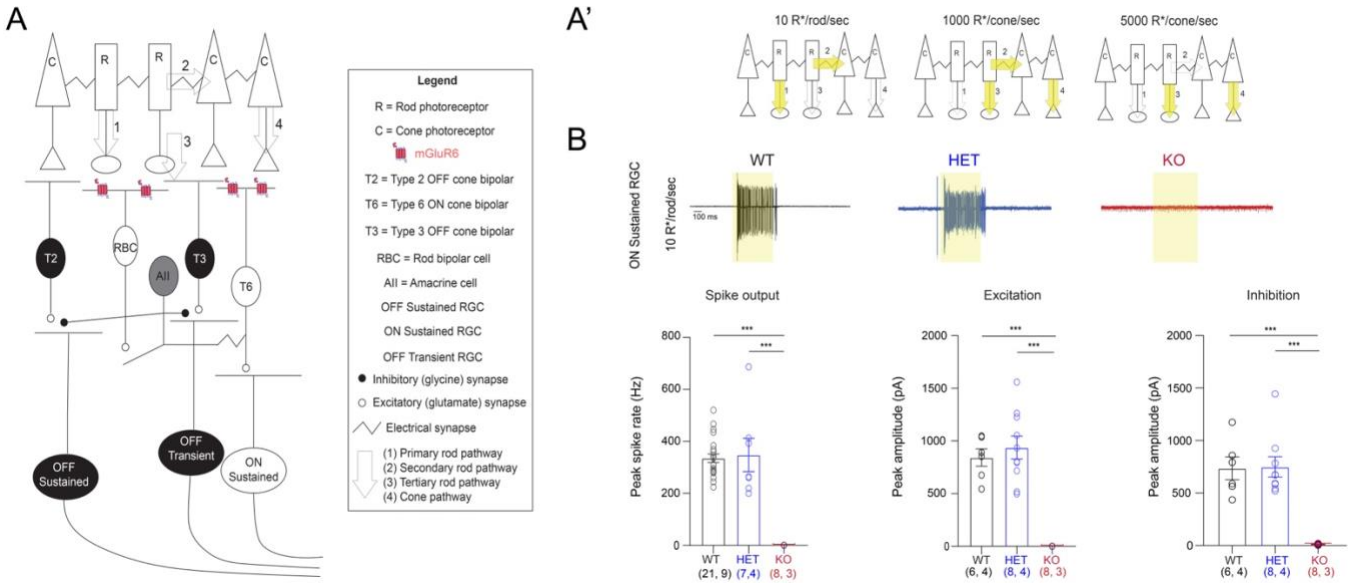

Figure 1. CSNB models selectively perturb the retinal ON pathway.

(A) Schematic of the mammalian retina illustrating pathways of visual information flow (1-4). Cells that depolarize to light increments constitute the ON pathway, whereas cells that depolarize to light decrements form the OFF pathway. The ON and OFF pathways diverge at the first synapse in the retina, where rods and cones transmit glutamate to rod and cone bipolar cells. ON bipolar cells express the metabotropic glutamate receptor mGluR6; OFF bipolar cells express ionotropic glutamate receptors. The AII amacrine cell bridges crosstalk between the two pathways, with glutamate release from rod bipolar cells and gap junctional coupling with ON cone bipolar cells governing the glycinergic output of AII amacrine cells to the OFF pathway. These signals are relayed to ON and OFF alpha retinal ganglion cells (RGCs), which generate and transmit action potentials to the cortex. Key output ganglion cells are the alpha ON sustained and OFF sustained and transient cells. We developed two models of congenital stationary night blindness (CSNB) with 50% (HET) or 100% (KO) suppression of ON pathway input in the outer retina, mediated by elimination of mGluR6. (**A'**) Different circuits are recruited across luminance levels (R* = photoisomerization events; summarized from calculations as per Jin et al.,[29]). At 10 R*/rod/sec, the 1º (rod → rod bipolar cell) and 2º (rod-cone gap junction) pathways are activated. At 1000 R*/S-cone/sec, the 2º, 3º (rod → OFF cone bipolar), and cone-mediated pathways are engaged. At 5000 R*/S-cone/sec, the 3º and cone-mediated pathways (4º) are active. (**B**) *Top:* Representative spike traces of ON sustained RGCs across the three genotypes at dim rod-light levels (response to 10 R*/rod/sec flash). *Bottom:* Bar graphs quantifying peak spike rate, peak amplitude of excitation and inhibition for ON sustained RGCs across genotypes. Note the complete suppression of light-

evoked excitation, inhibition, and spike output in KO cells, whereas HET RGCs show no significant differences compared to wildtype (WT) RGCs. Numbers in parentheses indicate the number of cells, animals. Data shown as mean ± SEM.

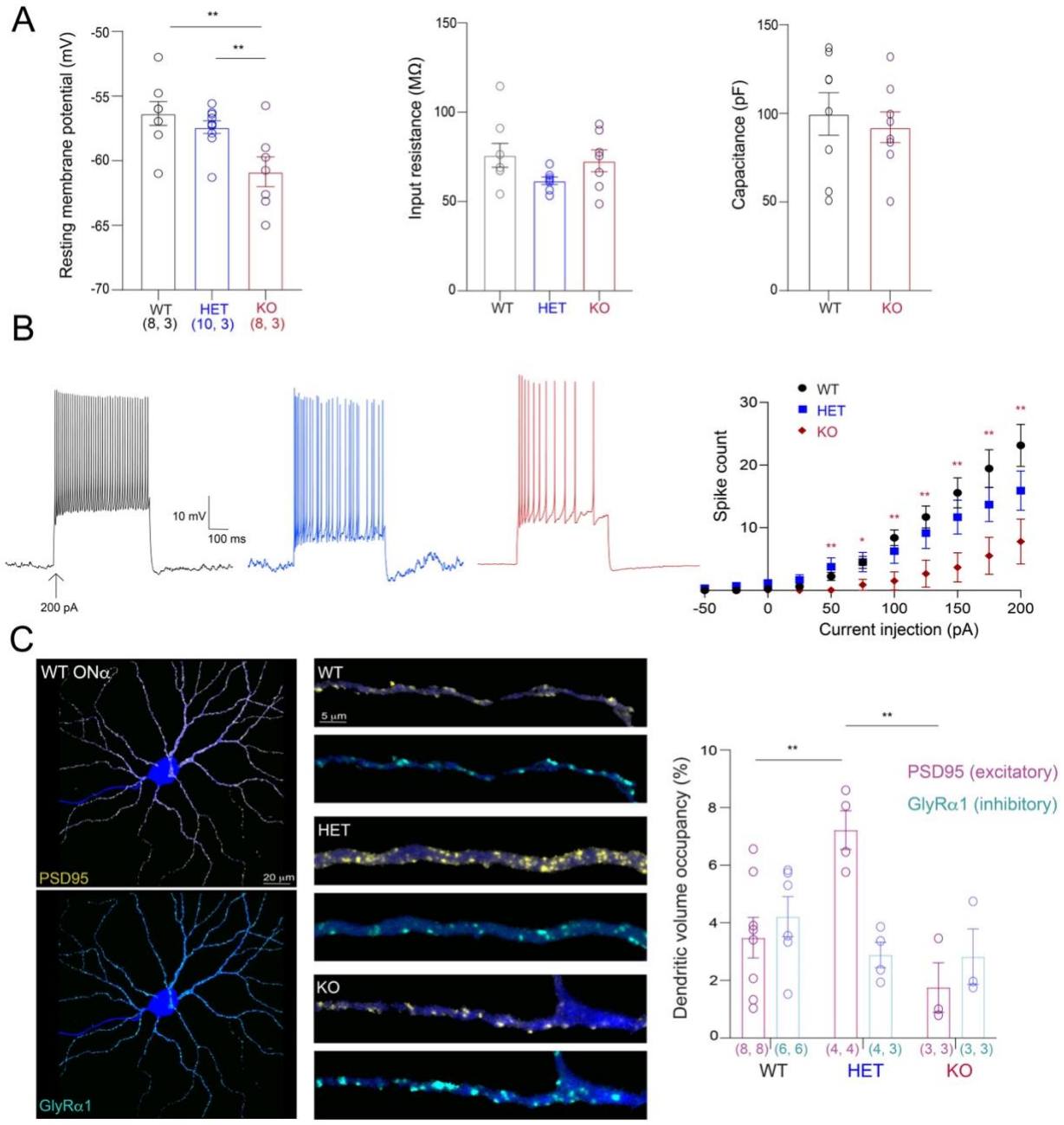

Figure 2. Differential recruitment of compensatory mechanisms in ON sustained RGCs after ON pathway suppression.

(**A**) Intrinsic properties of ON sustained RGCs across genotypes (WT: black, HET: blue, KO: red). The resting membrane potential is significantly hyperpolarized in KO cells compared to WT and HET ON sustained RGCs. Input resistance and cellular capacitance, calculated via voltage response to hyperpolarizing current injections, are unchanged in the KO. (**B**) *Left:* Exemplar trace of WT, HET and KO ON sustained RGC spiking in response to 200pA current injections. *Right:* Quantification of the ON sustained

spike count in response to current injections across genotypes. Despite deafferented ON sustained RGCs in the KO, the cells remain capable of spiking independently of light input, although the spike output is significantly reduced compared to WT. (**C**) Representative image of neurobiotin-filled ON sustained RGC with PSD95 (yellow) and GlyRa1 (cyan) immunolabeling signals within the dendrites. *Right*: Quantifications of the percentage volume occupancy of the synaptic markers within ON alpha arbors across genotypes. Immunohistochemical analysis of excitatory (PSD95) and inhibitory (GlyRa1) synaptic proteins within the dendrites of ON sustained RGCs reveals upregulation of the excitatory synaptic marker PSD95 in HET retinas, revealing a potential compensation for reduced upstream excitatory drive. Numbers in parentheses indicate the number of cells, animals. Data shown as mean ± SEM.

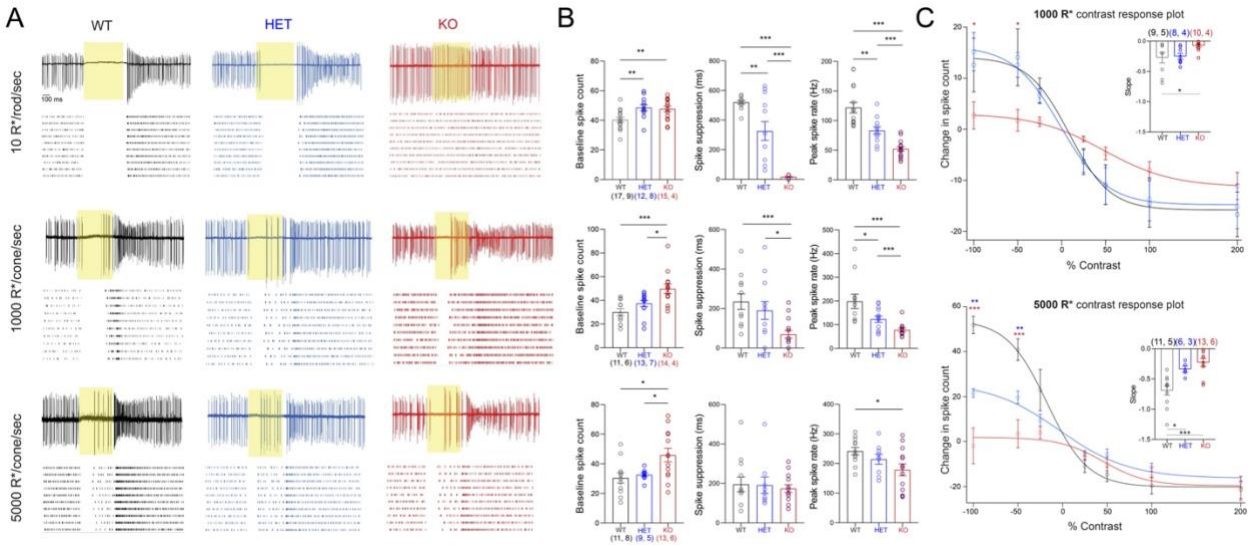

Figure 3. Differential luminance-dependent dysfunction in the CSNB OFF RGC pathway across the two models (HET vs. KO).

(**A**) Representative spike traces and raster plots of OFF sustained RGCs across each luminance level are shown. Note that KO OFF sustained RGCs are unable to suppress spikes during dim (10 R*/rod/sec) light flashes, unlike OFF sustained RGCs in WT and HET retinas. (**B**) Bar plot quantifications of baseline spiking (pre-stimulus), period of spike suppression (during stimulus), and peak spike rate (post-stimulus) for OFF sustained RGCs across genotypes and luminance conditions. The HET RGCs displays spiking deficits predominantly at the lowest luminance level (response to 10 R*/rod/sec flash), whereas the KO RGCs exhibit persistent deficits across all luminance levels. The encoding capability of HET and KO OFF sustained RGCs improves as luminance increases, consistent with the CSNB phenotype. (**C**) Contrast response plots of OFF sustained RGCs at 1000 R*/cone/sec and 5000 R*/cone/sec across genotypes. *Inset:* Slope quantifications from -50 to +25% contrast are shown across genotypes for each luminance level. Assessment of cellular contrast sensitivity demonstrates contrast deficits for HET OFF sustained RGCs at bright light levels. Note the complete inability of KO cells to encode contrasts across luminance levels. Numbers in parentheses indicate the number of cells, animals. Data shown as mean ± SEM.

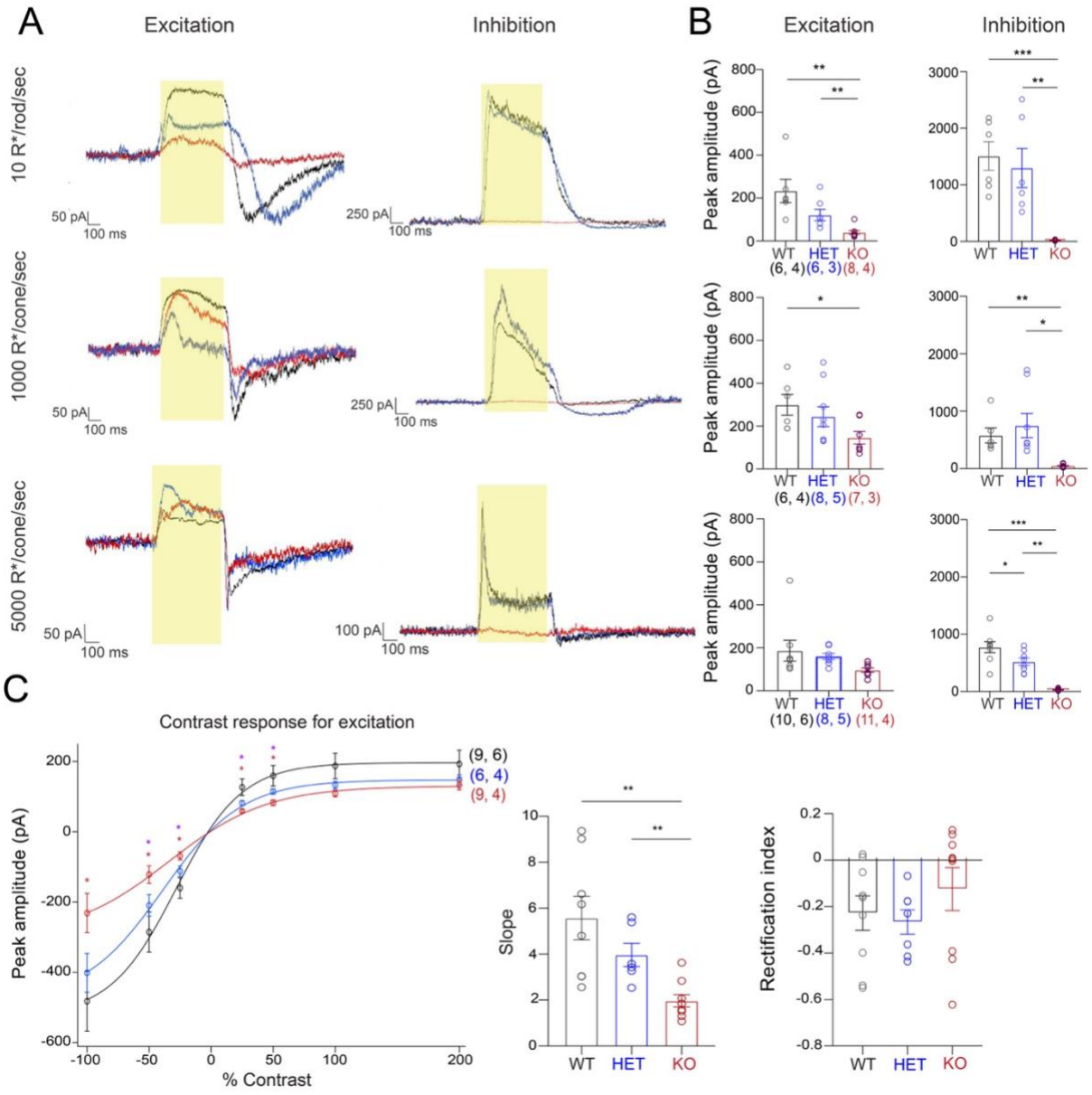

Figure 4. Synaptic imbalance across light levels in CSNB OFF pathway RGCs causes deficits in contrast encoding.

(**A**) Representative traces of excitatory and inhibitory synaptic currents for OFF sustained RGCs across genotypes and luminance levels. Note that for these RGCs excitation occurs at light offset (OFF pathway), and inhibition occurs during light onset (ON pathway). (**B**) Quantification of peak response amplitudes across light levels shows that KO OFF sustained RGCs receive little to no inhibitory synaptic input across all light levels. At the highest luminance, there are no significant differences in excitation across genotypes. (**C**) Excitatory contrast response plot at 5000 R*/cone/sec for OFF sustained RGCs across genotypes. *Right*: Quantification of response slope from -50 to +25 contrast

and quantification of rectification index of OFF sustained RGCs across genotypes from -50 to +50 contrast. Despite normal excitation at 5000 R*/cone/sec, KO OFF sustained RGCs exhibit significant deficits in excitatory contrast encoding. Numbers in parentheses indicate the number of cells, animals. Data shown as mean ± SEM.

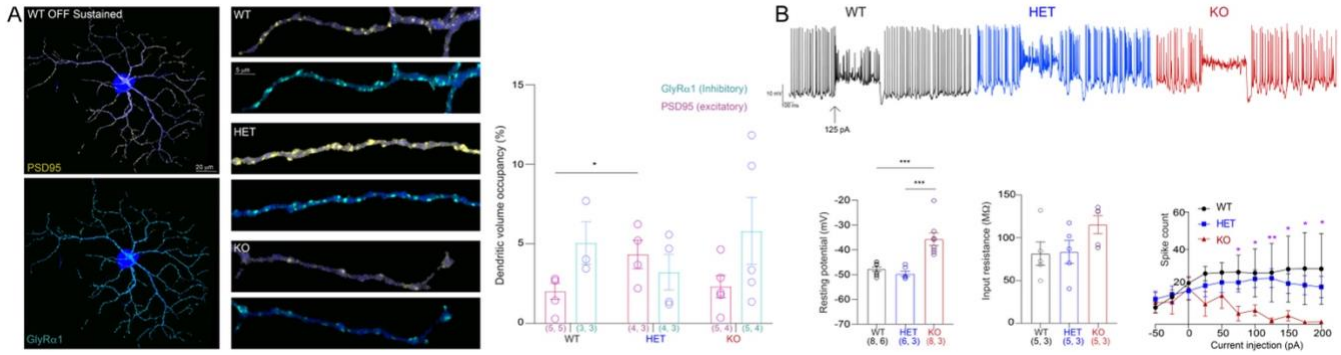

Figure 5. OFF pathway RGCs engage distinct compensatory mechanisms upon ON pathway disruption.

(**A**) *Left:* Representative image of neurobiotin-filled OFF sustained RGCs with PSD95 (yellow) and GlyRa1 (cyan) immunolabeling signal within dendrites. *Right:* Higher magnification view of PSD95 and GlyRa1 signal within dendrites of OFF sustained RGCs across genotypes. *Right*: Quantification of percent volume occupancy of synaptic proteins within OFF sustained dendrites across genotypes. Immunohistochemical analysis showed upregulation of excitatory synaptic protein PSD95 across arbors of HET OFF sustained RGCs. (**B**) *Top:* Exemplar traces of WT (black), HET (blue) and KO (red) OFF sustained RGCs in response to 125pA current injection. *Bottom:* Quantifications of resting membrane potential, input resistance, and spike count in response to current injection for OFF sustained RGCs across genotypes. KO OFF sustained RGCs have altered intrinsic excitability, shifting the resting potential to a more depolarized state compared to WT and HET RGCs. The input resistance, however, is unaffected in the KO. Serial current injections reveal that increased excitability results in progressive reduction in spike output due to depolarization block in the KO. Numbers in parentheses indicate the number of cells, animals. Data shown as mean ± SEM.

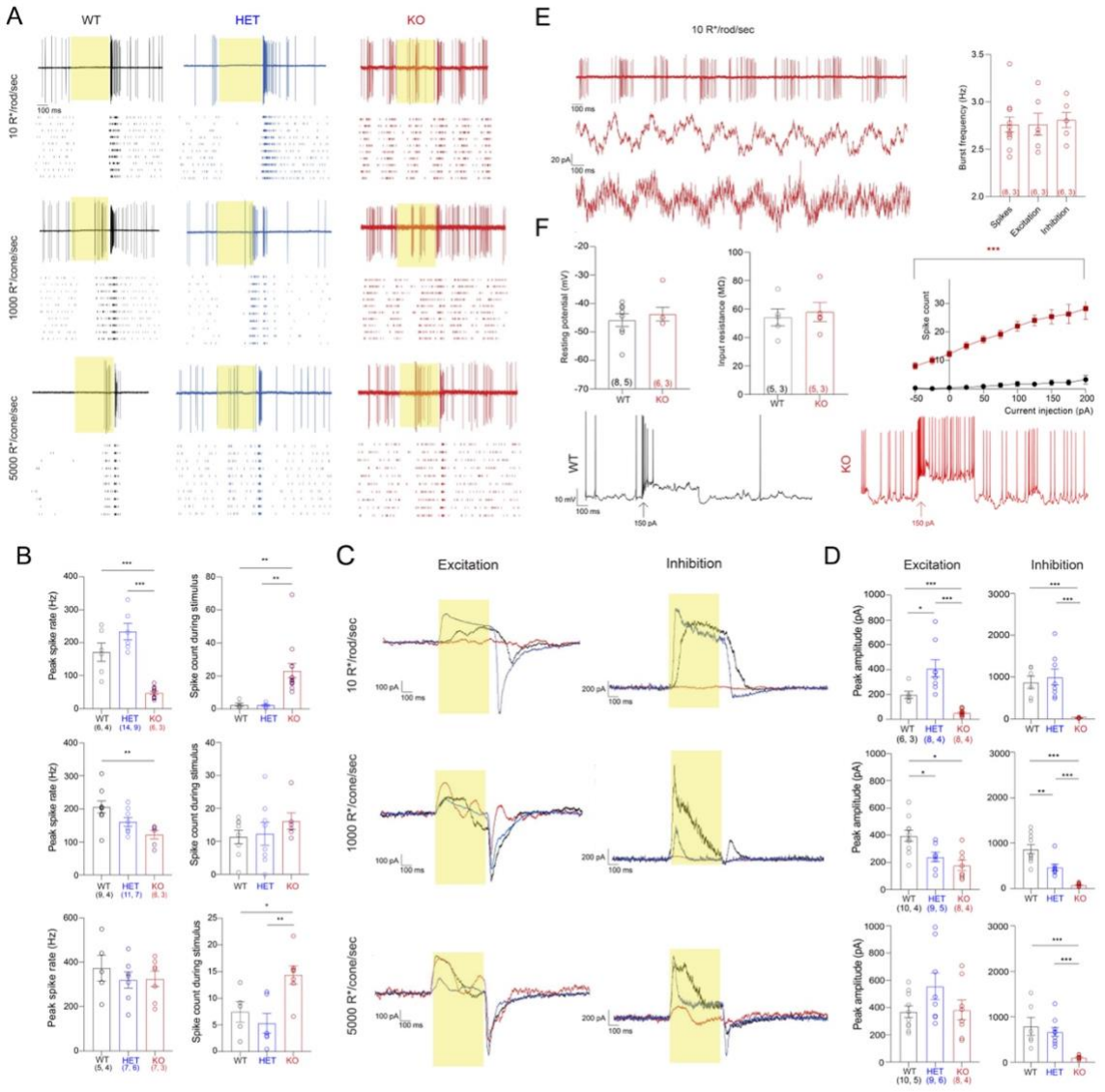

Figure 6. OFF transient RGCs display burst-like aberrant activity in the KO CSNB model, impairing their OFF response profiles and coding capabilities.

(**A**) Representative spike traces and raster plots for OFF transient RGCs across luminance and genotypes. Note the spike burst phenotype in KO OFF transient RGCs, most prominent at low luminance and persistent across luminance levels. (**B**) Bar plot quantifications of peak spike rate at light offset and spike count during light stimulus reveals aberrant elevated spiking of KO RGCs during the light stimulus. (**C**) Representative excitatory and inhibitory current waveforms across luminance levels and genotypes for OFF transient RGCs. (**D**) Quantifications of peak excitatory and inhibitory current amplitudes across luminance levels and genotypes. Quantifications show that KO cells receive little to no inhibitory input across all light levels and have reduced excitatory input, which improves as luminance increases. (**E**) Representative spike trace and

excitatory and inhibitory oscillatory bursts at 10 R*/rod/sec for the KO OFF transient RGCs. *Right*: Quantification of burst frequency which is approximately 3 Hz, and distinct from the frequency of degeneration-related bursts (see text for details). (**F**) *Top:* Quantification of resting membrane potential, input resistance, and spike count in response to current injections for the WT and KO OFF transient RGCs. *Bottom:* Exemplar traces of WT and KO OFF transient RGC spike output in response to 150 pA current injection. Passive intrinsic properties are not impaired in KO OFF transient RGCs, but there is an increase in overall spiking in response to current injection compared to WT, suggesting potential alterations in the active properties of KO OFF transient RGCs (see text for details). Numbers in parentheses indicate the number of cells, animals. Data shown as mean ± SEM.

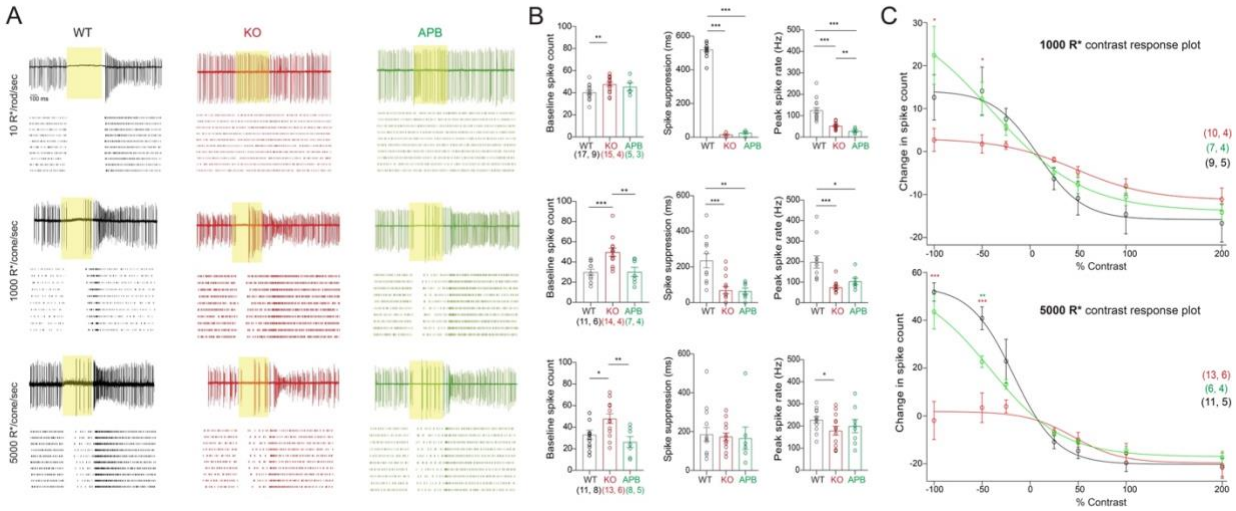

Figure 7. OFF pathway RGCs cope better with transient rather than chronic blockade of ON pathway input.

(**A)** Exemplar spike traces and raster plots for the WT (black), KO (red), and APB-treated (green) OFF sustained RGCs across luminance levels. Comparison of spike traces and raster plots generated from genetic versus pharmacologic blockade of the ON pathway shows similarity in the profile of spike suppression during the light step. However, the elevated baseline spiking seen in KO RGCs is not observed in APB-treated RGCs. (**B**) Quantifications of baseline spiking, period of spike suppression during light stimulation, and peak spike output at light offset for OFF sustained RGCs across conditions. Spike suppression capability of the OFF sustained RGCs is the same in both the genetic and pharmacologic blockade. (**C**) Contrast response plots at 1000 R*/cone/sec and 5000 R*/cone/sec for the OFF sustained RGCs comparing WT, KO, and APB-treated conditions. The contrast encoding capability of OFF sustained RGCs is better following transient blockade of the ON pathway with APB. Numbers in parentheses indicate the number of cells, animals. Data shown as mean ± SEM.

Appendix

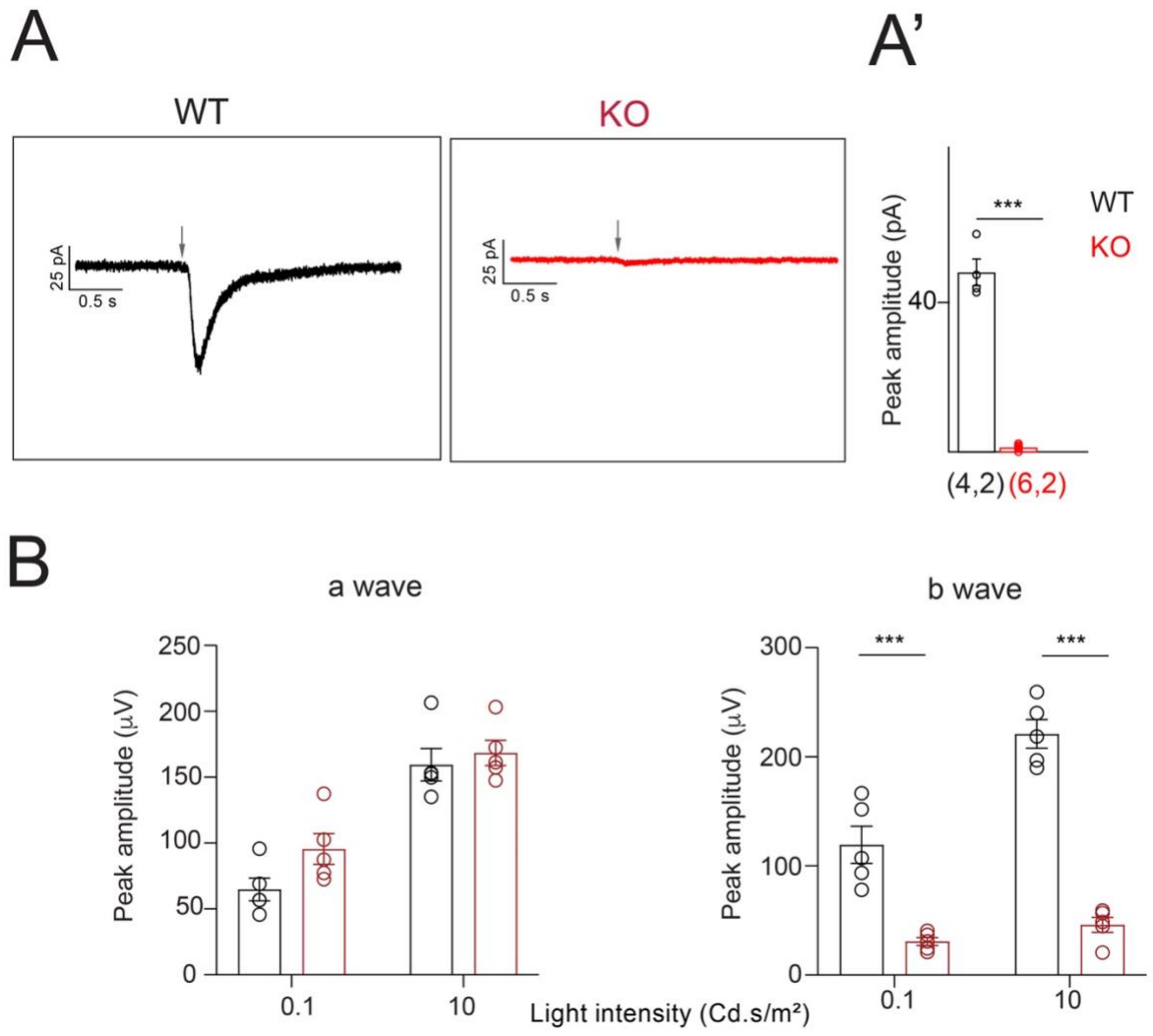

Figure S1 (related to Figure 1): Complete suppression of mGluR6-mediated photoreceptor input in the KO.

(**A**) Precise application of CPPG, an mGluR6 antagonist, at the dendrites of rod bipolar cells causes depolarization in WT rod bipolar cells but not KO rod bipolar cells. The lack of response in the KO confirms the absence of mGluR6 surface expression. Numbers in parentheses indicate the number of cells, animals. (**B**) Scotopic electroretinography quantifications show absence of the b-wave in KO mice, indicating that the ON pathway is functionally silent, whereas the presence of a comparable a-wave across genotypes confirms normal photoreceptor function. N = 5 animals per genotype. Data shown as mean ± SEM.

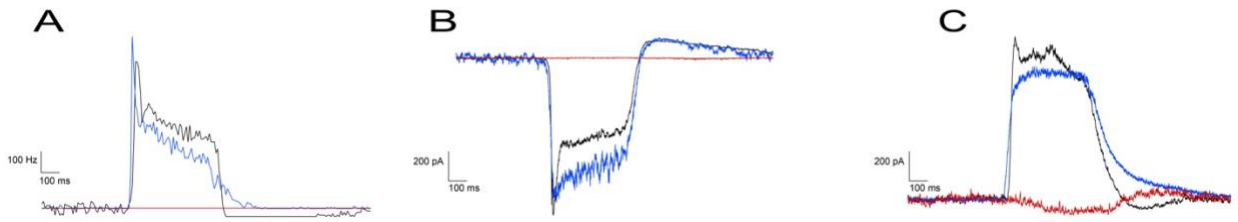

Supplemental Figure 2 (related to Figure 1): Exemplar traces recorded from ON sustained RGC shows similar response patterns between WT and HET.

(**A**) Representative peri-stimulus time histogram (PSTH) from an ON sustained RGC to a 10 R*/rod/sec flash in WT (black), HET (blue) and KO (red) retina confirming the elimination of ON pathway signals in the KO.

(**B**) Exemplar excitatory current responses (10 R*/rod/sec) of ON sustained RGC in WT, HET and KO retinas. Note the lack of responses in the KO as expected and comparable response profiles between the HET and WT.

(**C**) Inhibitory current exemplars in response to a 10 R*/rod/sec light flash from darkness in WT, HET and KO retinas.

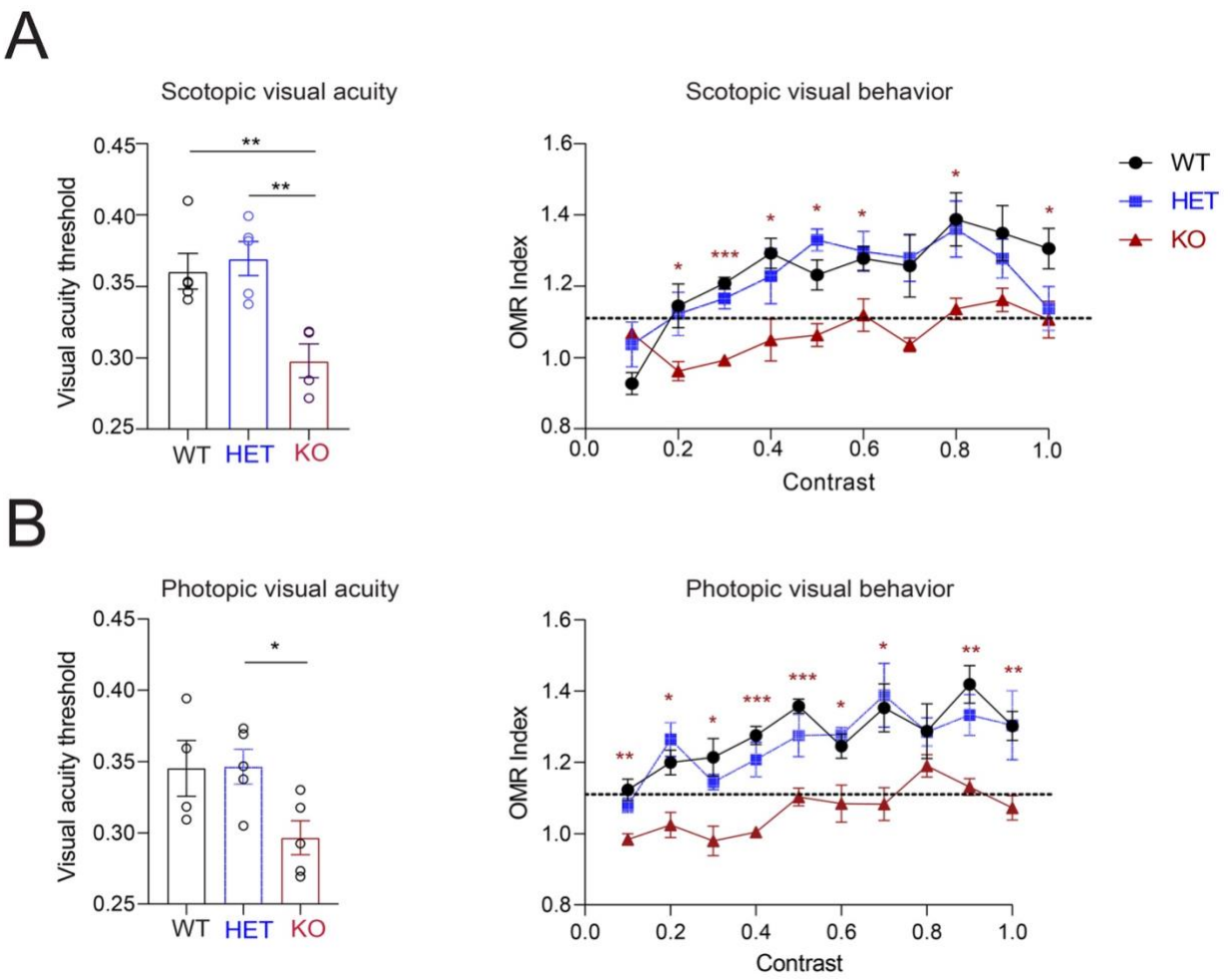

Supplemental Figure 3 (related to Figures 3–5): Optomotor response assay shows severe visual impairment in KO mice and normal responses in HET mice.

(**A**) Visual acuity and contrast sensitivity under dim light conditions are significantly reduced in KO (red) mice compared to both WT (black) and HET (blue) mice. Data shown as mean ± SEM.

(**B**) Visual acuity and contrast sensitivity under bright light conditions reveal that KO mice have impaired visual behavior even under daylight conditions. Note: the cellular contrast response plots for OFF sustained RGCs mirror the behavioral contrast sensitivity findings. N = 5 animals per genotype. Data shown as mean ± SEM.

Author Contributions: JK performed the electrophysiological, immunohistochemical, and behavioral experiments and analyses. **AS** aided in the early electrophysiological experiments. **SG** wrote custom MATLAB scripts to facilitate analyses. **PKS** aided in the ERG experiments. **BRP** provided feedback on ERG experimental design and data collections. **RS** provided feedback on all experiments and experimental design and carried out the CPPG puff whole-cell recordings from rod bipolar cells in the WT and KO models. **MH** generated the two CRISPR-mediated mutant mouse lines, provided feedback on experimental design, experiments, and analyses, and aided in the immunohistochemical experiments.

Chapter 3: Discussion

Context-dependent Recruitment of Homeostatic Plasticity Mechanisms

Our study reveals that the extent of ON pathway suppression in the mammalian retina critically determines whether neuroplasticity mechanisms become adaptive or maladaptive. In the HET model, where mGluR6 is partially (~50%) eliminated, the retina mounts adaptive responses that largely preserve visual function. Notably, the upregulation of excitatory synaptic proteins in HET ON sustained retinal ganglion cells (RGCs) compensates for reduced excitatory drive at the first synaptic layer, underscoring the retina's remarkable capacity to adjust synaptic strength and maintain signal transmission with diminished input.

Supporting this concept, prior work using diphtheria toxin systems to partially ablate photoreceptors or bipolar cells reveals context-dependent homeostatic plasticity. For example, partial rod photoreceptor ablation reduces excitatory output, prompting a compensatory reduction in inhibitory input to rod bipolar cells, thus stabilizing network excitability through a different approach than we observed (Care et al., 2020). Similarly, partial cone ablation triggers dendritic remodeling in cone bipolar cells, facilitating new synaptic contacts with surviving cones to preserve the receptive fields of ON sustained ganglion cells (Care et al., 2019). Even during cone outer segment degeneration, inner segments maintain some light transmission, suggesting ongoing ion channel and photopigment trafficking adjustments (Ellis et al., 2023). More severe disruptions, such as rod and ON cone bipolar cell ablation, also induce dendritic remodeling, with remaining bipolar cells extending neurites to sustain retinal output (Johnson et al., 2017). However,

computational models of photoreceptor degeneration suggest that any reorganization following deafferentation may be inherently destabilizing, cross-wiring circuits in ways that ultimately corrupt signal fidelity (Marc and Jones, 2003). This concept aligns with observations in advanced retinitis pigmentosa, where extreme photoreceptor loss surpasses the retina's adaptive capacity. The result is non-specific ganglion cell hyperexcitability and oscillatory spike bursts, which may underlie maladaptive visual hallucinations such as Charles Bonnet syndrome (O'Hare et al., 2015).

Our KO model, representing complete mGluR6 elimination, mirrors this maladaptive trajectory. Visual behavior assays confirm that KO animals are functionally blind under a range of luminance levels. Intrinsic property changes—such as the depolarized resting membrane potential in KO OFF sustained RGCs—reflect neuronal attempts to adjust excitability in response to chronic input deprivation. But these alterations elevate baseline spiking and impair contrast sensitivity, a hallmark function of OFF sustained cells. Notably, KO OFF transient RGCs display aberrant ~3 Hz oscillatory spike bursts, absent in neighboring OFF sustained RGCs despite similar input imbalances. This specificity points to a mechanism unique to OFF transient RGCs, potentially driven by distinct presynaptic OFF bipolar subtypes (Yu et al., 2018). Indeed, excitatory inputs to OFF transient RGCs mirror the ~3 Hz oscillatory signature. Though oscillations appear in rd1 and rd10 retinal degeneration models (Margolis et al., 2014; Biswas et al., 2014), their broader cell-type involvement and differing oscillation frequencies contrast with the selective ~3 Hz bursts we observe solely in KO OFF transient RGCs.

At the intrinsic level, our current-clamp recordings show that KO OFF transient RGCs do not exhibit a shifted resting membrane potential capable of producing spike bursts. Yet, these cells respond to current injections with dramatically increased spiking, without showing burst behavior under those conditions. This observation suggests that KO OFF transient RGCs may rely on active intrinsic property changes, such as altered ion channel expression, rather than passive shifts in resting potential. Supporting this idea, changes in ion channel expression can shape RGC spike output patterns differently between cells receiving identical synaptic input (Wienbar and Schwartz, 2022), and earlier work indicates that the light-evoked bursts of OFF transient RGCs are sensitive to T-type calcium channel antagonists (Murphy and Rieke, 2011).

To clarify whether dysfunctional responses such as elevated baseline spiking in OFF sustained RGCs and oscillatory bursts in OFF transient RGCs stem from plasticity or ON pathway suppression, we incubated retinas in APB to transiently block the ON pathway and then replicated our KO recordings. In APB-treated retinas, intrinsic properties remain largely normal. Baseline spiking elevations normalized under most light conditions, and OFF transient RGCs did not generate oscillatory spike bursts. However, both APB-treated and KO OFF sustained RGCs failed to suppress spiking effectively during dim-to-moderate light stimulation, implying an increased reliance on the ON pathway for inhibitory input at lower luminance, which is supported by other previous studies (Manookin et al., 2008; Murphy and Rieke, 2011). At bright-light levels, their spiking profiles are nearly indistinguishable from wild-type levels, indicating that OFF RGC output depends on ON-derived inhibition primarily in darker environments.

Maladaptive compensations expose the retina's limitations in preserving function under extreme disruptions, raising the question of how plasticity mechanisms are selectively engaged. Broadly, homeostatic plasticity can arise from either activity-dependent or cell-density-dependent triggers (Turrigiano, 2012; Fitzpatrick and Kerschensteiner, 2023). While prior diphtheria toxin studies (Care et al., 2020, 2019; Johnson et al., 2017; Lee et al., 2022) illustrate cell-density-dependent triggers, our findings align with activity-dependent triggers: the ON pathway's level of activity dictates whether compensations become beneficial or detrimental. Intriguingly, the inner retina retains significant plasticity after maturation; for example, light exposure following prolonged visual deprivation can drive molecular maturation of GABAergic synapses at bipolar cell axons (Wisner et al., 2023). Other work using tetanus toxin to silence photoreceptor glutamate release reveals that proper molecular organization of ON pathway constituents, including mGluR6 localization, depends on sustained neurotransmission (Cao et al., 2015). Thus, activity-dependent cues are vital for shaping maturing retinal circuits, though it remains unclear why partial versus complete ON pathway suppression selectively recruits synaptic or intrinsic compensations.

The contrasting outcomes between HET and KO CSNB models suggest that a critical threshold of ON pathway activity is needed to engage adaptive rather than maladaptive mechanisms. Below this threshold, neurons may resort to intrinsic changes that fail to restore function, as observed in the KO model. Why do partial and complete ON pathway suppression recruit different compensations? In principle, neurons can shift the synaptic input–output curve either by scaling synaptic expression (Turrigiano et al., 1998) or by modulating intrinsic excitability (Desai et al., 1999). Our findings in alpha

RGCs imply that the extent of input loss shapes which compensatory mechanism dominates, aligning with theoretical models predicting context-dependent recruitment (Turrigiano, 2011). This phenomenon also appears in auditory systems, where complete cochlear deafferentation leads to altered intrinsic properties in cortical circuits (Xu et al., 2007; Kotak et al., 2005).

Our work clarifies the cellular and synaptic basis of adaptive and maladaptive responses to partial and complete ON pathway suppression. Historically, mGluR6 knockout mice have offered insight into ON pathway function. Indeed, early studies showed that ON responses were eliminated in the superior colliculus of these mutants, while OFF responses remained (Masu et al., 1995). They also lacked the ERG b-wave, paralleling our observations (Masu et al., 1995; Dryja et al., 1993). Surprisingly, shuttle box avoidance testing revealed no obvious visual deficits, suggesting possible OFF pathway compensation (Masu et al., 1995). Later work using optokinetic nystagmus (OKN) or optomotor response (OMR) assays, however, identified reductions in both visual acuity and contrast sensitivity across luminance levels (Pinto et al., 2007; Iwakabe et al., 1997). Further research noted that, in some tasks, OFF circuitry can partially offset the loss of ON input. For instance, eliminating mGluR6 did not reduce forced-choice visual performance (Beier et al., 2022). These inconsistencies likely stem from the distinct visual features tested: the shuttle box assay taps more complex visual processing, whereas OKN and OMR heavily depend on motion detection and contrast sensitivity, functions closely tied to the ON pathway.

Future Directions

While not all heterozygous gene deletions yield exactly ~50% protein expression, our preliminary data confirm this is roughly the case in our heterozygous model. Moving forward, we aim to deepen our understanding of the divergent mechanisms underlying adaptive synaptic scaling versus maladaptive intrinsic changes. For instance, if partial ON pathway suppression indeed upregulates excitatory synaptic proteins in ON ganglion cell dendrites, we expect elevated amplitude and frequency of spontaneous excitatory postsynaptic currents (sEPSCs). A related question is whether this upregulation manifests as a greater number of synapses or an increase in synaptic size. We will address this by coupling sEPSC recordings with advanced analyses of excitatory synapse number and distribution in the partial input suppression model, further refining our picture of the adaptive processes at work.

Additionally, an outstanding question regarding the source of oscillatory spike bursts remains unanswered. Based on our findings pointing to alterations in active intrinsic properties and previous literature implicating T-type calcium channels in spike generation of OFF transient RGCs, future experiments can combine immunohistochemistry and electrophysiology with pharmacology to address the role of ion channels. For the immunohistochemistry, one could principally target the expression of sodium channels clustered in the axon initial segment, where action potential generation is initiated. Differences in density, distribution, or subtypes of sodium channels might clarify the curious finding of hyperexcitability with normal resting membrane potential. Moreover, pharmacology using drugs such as Mibefradil, a calcium channel antagonist that selectively blocks T-type calcium channels, can be used to test the

hypothesis that overactivation of these channels may underlie the oscillatory burst activity (Murphy and Rieke, 2011).

Because our work has focused primarily on postsynaptic changes, one could also address the alterations on the presynaptic compartment in response to input suppression. Do the ribbon synapses of ON and OFF bipolar cells differ under partial versus complete ON pathway loss? Future experiments can examine whether bipolar cell glutamatergic ribbon structures undergo remodeling in response to input suppression. By co-labeling bipolar cell terminals for ribbons and comparing their density, size, and distribution between mutants and wild-type controls, one can determine whether the observed postsynaptic alterations coincide with presynaptic restructuring. To this end, one can also combine immunohistochemistry and serial blockface scanning electron microscopy analyses to enable detailed assessments of bipolar cell synapses.

These future directions become most tractable with a well-established working model. The model we propose applies additional insights as published in Khoussine et al., 2025 and works as follows. With 50% suppression of the photoreceptor to ON bipolar cell input stream, we find elevation in excitatory synaptic protein expression density on the dendrites of both ON and OFF alpha ganglion cells. Our findings do not indicate that the ON bipolar cells undergo alteration. This is evidenced by the 50% reduction in signal generation from ON bipolar cells that bear 50% mGluR6 expression as well as the absence of alterations to the ribbon synaptic terminal. We pinpoint the upregulation to the retinal ganglion cells through both the immunohistochemical evidence of increased PSD95 expression as well as through increased spontaneous excitatory post-synaptic currents (sEPSCs), which correlate structure with function. Through this schema, the

retina can maintain signal output fidelity and endure near-normal signal transmission and visual behavior despite the 50% reduction of input suppression.

Importantly, it is the partial nature of the input suppression which enables recovery of visual behavior. In our model with 100% reduction of photoreceptor to ON bipolar cell input, no such adaptive compensatory measures were noted that support normal visual behavior. Indeed, the animals lacking mGluR6 expression altogether are effectively blind across luminance conditions. The complete input suppression does not provide a substrate for adaptive compensation; though, there are certainly changes observed in the ganglion cells. Specifically, the ganglion cells in both the ON and OFF pathways undergo intrinsic property modifications that render their function inert or hyperactive, respectively. Neither compensation encourages normal visual function or behavior, and in this manner, have been determined to be maladaptive in effect. A permissive signal delivered in the right temporal context is needed to drive adaptive mechanisms, and the complete input suppression model lacks this drive.

Implications of Plasticity for Clinical Diagnostics and Therapeutics

Patients with CSNB due to mutations in the *GRM6* gene often present with night blindness, reduced or normal visual acuity, high myopia, photophobia, and pendular nystagmus (Zeitz et al., 2015; Dryja et al., 1993). Because these mutations follow autosomal recessive inheritance and may not lead to a complete absence of mGluR6, many patients may experience partial loss of function, permitting some ON pathway activity. This intermediate state aligns more closely with our HET model, but not entirely with our KO mice, which showed significant blindness in behavioral assays across both dim- and bright-light conditions. Of course, one must be careful when comparing mice

and humans. Mice are nocturnal, rod-dominant, and lack a fovea. In primates, the fovea is a specialized region of the macula responsible for high-acuity tasks like reading, populated solely by cone photoreceptors at its center (Sinha et al., 2017). Both ON and OFF parallel circuits are present in the fovea, and ON bipolar cells there also express mGluR6 (Vardi et al., 2000). Therefore, the foveal ON pathway is likely suppressed in complete CSNB. This raises a puzzling question: how do individuals with complete CSNB, who have limited peripheral and foveal ON signaling, still maintain near-normal vision in daylight? First, there could be subthreshold electrical signaling that the b-wave on scotopic ERG cannot sufficiently resolve. In such a case, it may be that these patients do retain partial ON pathway activity that consequently engage homeostatic mechanisms akin to those observed in our HET model, which permit enough signal transmission for functional vision under bright conditions. Under starlight, however, photon levels may be too sparse for such compensations to sustain vision, leading to night blindness. In practice, the degree of residual ON activity and the effectiveness of neuroplasticity both likely vary from patient to patient, producing a wide range of visual experiences as environmental luminance gradually diminishes to darkness. By comparing mouse and human retinas, we gain perspective on how partial mGluR6 function and circuit-level adaptations might explain the diverse clinical presentations of CSNB.

Throughout this thesis, retinitis pigmentosa (RP) and congenital stationary night blindness (CSNB) have been juxtaposed as conditions that each elicit homeostatic plasticity in the retina. Both disorders are inherited, making gene therapy a particularly promising avenue, but timing of intervention and extent of recovery remain crucial factors in determining its success. Recent findings in transgenic mice suggest that once

photoreceptor degeneration surpasses 50%, therapeutic correction becomes challenging (Scalabrino et al., 2023). How does this translate to human pathology? Luxturna, the first FDA-approved therapy for *RPE65*-related RP, produced improvements in visual performance that lasted at least four years (Wu et al., 2023), although patient outcomes varied based on the degree of photoreceptor loss at treatment onset. Intriguingly, canine models of CSNB with *LRIT3* mutations regained scotopic vision with only about 30% recovery of ON pathway function, as measured by electroretinography (Miyadera et al., 2022). These varied responses highlight that the threshold for restoring vision may differ from one condition or gene to another, underscoring the importance of pinpointing the optimal window for intervention.

While current approaches to estimate retinal structure and function in the course of disease and in response to treatment are grossly effective, both pathology and therapy alike ultimately act on the cellular level. To measure what matters and to measure it well are key tenets of shrewd clinical medicine. The barriers are many to achieve this resolution reliably at the scale needed for clinical adoption, yet adaptive optics imaging technology has provided a new lens to measure the living human retina at cellular resolution. It is being used routinely for clinical research and rapidly adapted for basic science, already revealing impactful insights into previously unexplained visual dysfunction in patients (Wu et al., 2017; Kolli et al, 2023). For retinitis pigmentosa, the confocal modality enabled through adaptive optics scanning light ophthalmoscopy (AOSLO) is particularly valuable.

To appreciate its potential impact, imagine a future in which a young patient presents to the inherited retinal degeneration clinic due to issues with night vision. This

could be either complete CSNB or early RP; fortunately, rapid availability of genetic testing clarifies a diagnosis of *RPE65*-related RP. The patient is a candidate for gene therapy and receives pre-treatment imaging with AOSLO, which maps the photoreceptor topography and quantifies photoreceptor density. Advances in optoretinography (ORG), the use of light stimulus to evoke and record photoreceptor function, coupled with AOSLO enable measurement of cellular structure and function at the margins of healthy cells and degenerating ones (Gong et al., 2024). Following treatment with gene therapy, the same retinal regions can be measured over time to determine response efficacy in addition to tests of visual performance. The inevitable phenotypic variations in response efficacy can be studied and used to determine whether there is a critical period of photoreceptor loss for effective gene therapeutic intervention. The hope for AOSLO imaging is earlier detection of microscopic cellular damage and improved measurement of the structures and functions that matter most in the retina for vision. One day, we might approach the timing of gene therapy the same way we do patching the good eye to prevent amblyopia. One of the great pleasures of completing my doctoral training at the University of Wisconsin-Madison is having learned alongside the physicians and scientists working in earnest to achieve this vision.

References

Abbott, S.B., and Nelson, S.B. (2000). Synaptic plasticity: taming the beast. *Nat Neurosci. 1178-83.* 10.1038/81453.

Ala-Laurila, P., and Rieke, F. (2014). Coincidence detection of single-photon responses in the inner retina at the sensitivity limit of vision. *Curr Biol* 24, 2888–2898. 10.1016/j.cub.2014.10.028.

Beier, C., Bocchero, U., Levy, L., Zhang, Z., Jin, N., Massey, S.C., Ribelayga, C.P., Martemyanov, K., Hattar, S., and Pahlberg, J. (2022). Divergent outer retinal circuits drive image and non-image visual behaviors. *Cell Rep* 39, 111003. 10.1016/j.celrep.2022.111003.

Biswas, S., Haselier, C., Mataruga, A., Thumann, G., Walter, P., and Muller, F. (2014). Pharmacological analysis of intrinsic neuronal oscillations in rd10 retina. *PLoS One* 9, e99075. 10.1371/journal.pone.0099075.

Bleckert, A., Parker, E.D., Kang, Y., Pancaroglu, R., Soto, F., Lewis, R., Craig, A.M., and Wong, R.O. (2013). Spatial relationships between GABAergic and glutamatergic synapses on the dendrites of distinct types of mouse retinal ganglion cells across development. *PLoS One* 8, e69612. 10.1371/journal.pone.0069612.

Botto, C., Rucli, M., Tekinsoy, M.D., Pulman, J., Sahel, J.A., and Dalkara, D. (2022). Early and late stage gene therapy interventions for inherited retinal degenerations. *Prog Retin Eye Res* 86, 100975. 10.1016/j.preteyeres.2021.100975.

Cao, Y., Sarria, I., Fehlhaber, K.E., Kamasawa, N., Orlandi, C., James, K.N., Hazen, J.L., Gardner, M.R., Farzan, M., Lee, A., *et al.* (2015). Mechanism for Selective Synaptic Wiring of Rod Photoreceptors into the Retinal Circuitry and Its Role in Vision. *Neuron* 87, 1248–1260. 10.1016/j.neuron.2015.09.002.

Care, R.A., Anastassov, I.A., Kastner, D.B., Kuo, Y.M., Della Santina, L., and Dunn, F.A. (2020). Mature Retina Compensates Functionally for Partial Loss of Rod Photoreceptors. *Cell Rep* 31, 107730. 10.1016/j.celrep.2020.107730.

Care, R.A., Kastner, D.B., De la Huerta, I., Pan, S., Khoche, A., Della Santina, L., Gamlin, C., Santo Tomas, C., Ngo, J., Chen, A., *et al.* (2019). Partial Cone Loss Triggers Synapse-Specific Remodeling and Spatial Receptive Field Rearrangements in a Mature Retinal Circuit. *Cell Rep* 27, 2171–2183.e5. 10.1016/j.celrep.2019.04.065.

Chichilnisky, E.J., and Kalmar, R.S. (2002). Functional asymmetries in ON and OFF ganglion cells of primate retina. *J Neurosci* 22, 2737–2747. 10.1523/JNEUROSCI.22-07-02737.2002.

Cooke, D., and Bear, M.F. (2010). How the mechanisms of long-term synaptic potentiation and depression serve experience dependent plasticity in primary visual cortex. Phil. Trans. R. Soc. B 369: 20130284. http://dx.doi.org/10.1098/rstb.2013.0284

Curcio, C.A., and Allen, R.R. (1990). Topography of ganglion cells in human retina. 300(1):5-25. 10.1002/cne.903000103.

DeVries, S.H. (2000). Bipolar cells use kainate and AMPA receptors to filter visual information into separate channels. *Neuron* 28, 847–856. 10.1016/s0896-6273(00)00158-6.

Demb, J.B., and Singer, J.H. (2012). Intrinsic properties and functional circuitry of the AII amacrine cell. *Vis Neurosci* 29, 51–60. 10.1017/S0952523811000368.

Desai, N.S., Rutherford, L.C., and Turrigiano, G.G. (1999). BDNF regulates the intrinsic excitability of cortical neurons. *Learn Mem* 6, 284–291.

Dryja, T.P., Berson, E.L., Rao, V.R., and Oprian, D.D. (1993). Heterozygous missense mutation in the rhodopsin gene as a cause of congenital stationary night blindness. *Nat Genet* 4, 280–283. 10.1038/ng0793-280.

Ellis, E.M., Paniagua, A.E., Scalabrino, M.L., Thapa, M., Rathinavelu, J., Jiao, Y., Williams, D.S., Field, G.D., Fain, G.L., and Sampath, A.P. (2023). Cones and cone pathways remain functional in advanced retinal degeneration. *Curr Biol* 33(8), 1513–1522.e4. doi: 10.1016/j.cub.2023.03.007.Fitzpatrick, M.J., and

Fitzpatrick, M.J., and Kerschensteiner, D. (2023). Homeostatic plasticity in the retina. *Prog Retin Eye Res* 94, 101131. 10.1016/j.preteyeres.2022.101131.

Goetz, G.A., and Palanker, D.V. (2016). Electronic approaches to restoration of sight. *Rep Prog Phys* 79, 096701. 10.1088/0034-4885/79/9/096701.

Gong, Z., Shi, Y., Liu, J., Sabesan, R. and Wang, R. K. (2024) Light-adapted flicker-optoretinography based on raster-scan optical coherence tomography towards clinical translation, *Biomedical Optics Express*, 15(10), pp. 6036–6051. doi: 10.1364/BOE.538481.

Grimes, W.N., Schwartz, G.W., and Rieke, F. (2014). The synaptic and circuit mechanisms underlying a change in spatial encoding in the retina. *Neuron* 82, 460–473. 10.1016/j.neuron.2014.02.037.

Grimes, W.N., Sedlacek, M., Musgrove, M., Nath, A., Tian, H., Hoon, M., Rieke, F., Singer, J.H., and Diamond, J.S. (2022). Dendro-somatic synaptic inputs to ganglion cells contradict receptive field and connectivity conventions in the mammalian retina. *Curr Biol* 32, 315–328.e4. 10.1016/j.cub.2021.11.005.

Hebb, D.O. (1949). The organization of behavior: a neuropsychological theory. New York: *John, Wiley & Sons.*

Hoon, M., Okawa, H., Della Santina, L., and Wong, R.O. (2014). Functional architecture of the retina: development and disease. *Prog Retin Eye Res* 42, 44–84. 10.1016/j.preteyeres.2014.06.003.

Hoon, M., Sinha, R., Okawa, H., Suzuki, S.C., Hirano, A.A., Brecha, N., Rieke, F., and Wong, R.O. (2015). Neurotransmission plays contrasting roles in the maturation of inhibitory synapses on axons and dendrites of retinal bipolar cells. *Proc Natl Acad Sci U S A* 112, 12840–12845. 10.1073/pnas.1510483112.

Hoon, M., Sinha, R., and Okawa, H. (2017). Using Fluorescent Markers to Estimate Synaptic Connectivity *In Situ*. In *Methods Mol Biol* 1538, 293–320. 10.1007/978-1-4939-6688-2_20.

Horton, J.C., and Sherk, H. (1984). Receptive field properties in the cat's lateral geniculate nucleus in the absence of on-center retinal input. *J Neurosci* 4, 374–380. 10.1523/JNEUROSCI.04-02-00374.1984.

Hubel, D.H., and Wiesel, T.N. (1963). Receptive fields of cells in striate cortex of very young, visually inexperienced kittens. *Journal of Neurophysiology* 26, 994–1002.

Ichinose, T., and Habib, S. (2022). ON and OFF Signaling Pathways in the Retina and the Visual System. *Front Ophthalmol (Lausanne)* 2. 10.3389/fopht.2022.989002.

Iwakabe, H., Katsuura, G., Ishibashi, C., and Nakanishi, S. (1997). Impairment of pupillary responses and optokinetic nystagmus in the mGluR6-deficient mouse. *Neuropharmacology* 36, 135–143. 10.1016/s0028-3908(96)00167-0.

Jiao, X., Ma, Z., Lei, J., Liu, P., Cai, X., Shahi, P.K., Chan, C.C., Fariss, R., Pattnaik, B.R., Dong, L., and Hejtmancik, J.F. (2021). Retinal Development and Pathophysiology in Kcnj13 Knockout Mice. *Front Cell Dev Biol* 9, 810020. 10.3389/fcell.2021.810020.

Jin, N., Zhang, Z., Keung, J., Youn, S.B., Ishibashi, M., Tian, L.M., Marshak, D.W., Solessio, E., Umino, Y., Fahrenfort, I., *et al.* (2020). Molecular and functional architecture of the mouse photoreceptor network. *Sci Adv* 6, eaba7232. 10.1126/sciadv.aba7232.

Johnson, R.E., Tien, N.W., Shen, N., Pearson, J.T., Soto, F., and Kerschensteiner, D. (2017). Homeostatic plasticity shapes the visual system's first synapse. *Nat Commun* 8, 1220. 10.1038/s41467-017-01332-7.

Katz, L.C., and Shatz, C.J. (1996). Synaptic activity and the construction of cortical circuits. Science 274, 1133–1138

Kolb, H., Linberg, K.A., and Fisher, S.K. (1992). Neurocircuitry of the cat retina: Analysis of the contacts between photoreceptors and bipolar, horizontal, and amacrine cells. *Journal of Comparative Neurology*. 318, 475–498

Kolli, A., Wong, J., Duret, S., Stewart, J.M., Roorda, A., Carroll, J., and Duncan, J.L. (2023). Outer retinal reflectivity changes with reduced visual function following anatomically successful repair of macula-off rhegmatogenous retinal detachment. *Investigative Ophthalmology & Visual Science*, 64(8):4334.

Kotak, V.C., Fujisawa, S., Lee, F.A., Karthikeyan, O., Aoki, C., and Sanes, D.H. (2005). Hearing loss raises excitability in the auditory cortex. *J Neurosci* 25, 3908–3918. 10.1523/JNEUROSCI.5169-04.2005.

Kramer, R.H., and Davenport, C.M. (2015). Lateral inhibition in the vertebrate retina: The case of the missing neurotransmitter. *PLoS Biology*, 13(12), e1002322. https://doi.org/10.1371/journal.pbio.1002322.

Kretschmer, F., Sajgo, S., Kretschmer, V., and Badea, T.C. (2015). A system to measure the Optokinetic and Optomotor response in mice. *J Neurosci Methods* 256, 91–105. 10.1016/j.jneumeth.2015.08.007.

Krieger, B., Qiao, M., Rousso, D.L., Sanes, J.R., and Meister, M. (2017). Four alpha ganglion cell types in mouse retina: Function, structure, and molecular signatures. *PLoS One* 12, e0180091. 10.1371/journal.pone.0180091.

Lamb, T.D. (2016). Why rods and cones? *Eye (Lond)* 30, 179–185. 10.1038/eye.2015.236.

Lee, J.Y., Care, R.A., Kastner, D.B., Della Santina, L., and Dunn, F.A. (2022). Inhibition, but not excitation, recovers from partial cone loss with greater spatiotemporal

integration, synapse density, and frequency. *Cell Rep* 38, 110317. 10.1016/j.celrep.2022.110317.

Liang, Z., and Freed, M.A. (2010). The ON pathway rectifies the OFF pathway of the mammalian retina. *J Neurosci* 30, 5533–5543. 10.1523/JNEUROSCI.4733-09.2010.

Madugula, S.S., Gogliettino, A.R., Zaidi, M., Aggarwal, G., Kling, A., Shah, N.P., Brown, J.B., Vilkhu, R., Hays, M.R., Nguyen, H., *et al.* (2022). Focal electrical stimulation of human retinal ganglion cells for vision restoration. *J Neural Eng* 19. 10.1088/1741-2552/aca5b5.

Maddox, D.M., Vessey, K.A., Yarbrough, G.L., Invergo, B.M., Cantrell, D.R., Inayat, S., Balannik, V., Hicks, W.L., Hawes, N.L., Byers, S., *et al.* (2008). Allelic variance between GRM6 mutants, Grm6nob3 and Grm6nob4 results in differences in retinal ganglion cell visual responses. *J Physiol* 586, 4409–4424. 10.1113/jphysiol.2008.157289.

Manookin, M.B., Beaudoin, D.L., Ernst, Z.R., Flagel, L.J., and Demb, J.B. (2008). Disinhibition combines with excitation to extend the operating range of the OFF visual pathway in daylight. *J Neurosci* 28, 4136–4150. 10.1523/JNEUROSCI.4274-07.2008.

Margolis, D.J., Gartland, A.J., Singer, J.H., and Detwiler, P.B. (2014). Network oscillations drive correlated spiking of ON and OFF ganglion cells in the rd1 mouse model of retinal degeneration. *PLoS One* 9, e86253. 10.1371/journal.pone.0086253.

Marco, S.D., Protti, D.A., and Solomon, S.G. (2013). Excitatory and inhibitory contributions to receptive fields of alpha-like retinal ganglion cells in mouse. *J Neurophysiol* 110, 1426–1440. 10.1152/jn.01097.2012.

Masland, R.H. (2001). The fundamental plan of the retina. *Nat Neurosci* 4, 877–886. 10.1038/nn0901-877.

Masu, M., Iwakabe, H., Tagawa, Y., Miyoshi, T., Yamashita, M., Fukuda, Y., Sasaki, H., Hiroi, K., Nakamura, Y., Shigemoto, R., *et al.* (1995). Specific deficit of the ON response in visual transmission by targeted disruption of the mGluR6 gene. *Cell* 80, 757–765. 10.1016/0092-8674(95)90354-2.

Majumdar, S., Heinze, L., Haverkamp, S., Ivanova, E., and Wassle, H. (2007). Glycine receptors of A-type ganglion cells of the mouse retina. *Vis Neurosci* 24, 471–487. 10.1017/S0952523807070174.

Maurer, D., Mondloch, C.J., and Lewis, T.L. (2007). Effects of early visual deprivation on perceptual and cognitive development. *Progress in Brain Research* 164, 87–104. https://doi.org/10.1016/S0079-6123(07)64005-9.

McCall, M.A., and Gregg, R.G. (2008). Comparisons of structural and functional abnormalities in mouse b-wave mutants. *J Physiol* 586, 4385–4392. 10.1113/jphysiol.2008.159327.

Miyadera, K., Santana, E., Roszak, K., Iffrig, S., Visel, M., Iwabe, S., Boyd, R.F., Bartoe, J.T., Sato, Y., Gray, A., *et al.* (2022). Targeting ON-bipolar cells by AAV gene therapy stably reverses LRIT3-congenital stationary night blindness. *Proc Natl Acad Sci U S A* 119, e2117038119. 10.1073/pnas.2117038119.

Morgan, J.L., Schubert, T., and Wong, R.O. (2008). Developmental patterning of glutamatergic synapses onto retinal ganglion cells. *Neural Dev* 3, 8. 10.1186/1749-8104-3-8.

Munch, T.A., da Silveira, R.A., Siegert, S., Viney, T.J., Awatramani, G.B., and Roska, B. (2009). Approach sensitivity in the retina processed by a multifunctional neural circuit. *Nat Neurosci* 12, 1308–1316. 10.1038/nn.2389.

Murphy, G.J., and Rieke, F. (2006). Network variability limits stimulus-evoked spike timing precision in retinal ganglion cells. *Neuron* 52, 511–524. 10.1016/j.neuron.2006.09.014.

Murphy, G.J., and Rieke, F. (2011). Electrical synaptic input to ganglion cells underlies differences in the output and absolute sensitivity of parallel retinal circuits. *J Neurosci* 31, 12218–12228. 10.1523/JNEUROSCI.3241-11.2011.

Neitz, M., and Neitz, J. (2000). Molecular genetics of color vision and color vision defects. *Archives of Ophthalmology* 118(5), 691–700. https://doi.org/10.1001/archopht.118.5.691.

Nawy, S. (2004). Desensitization of the mGluR6 transduction current in tiger salamander On bipolar cells. *J Physiol* 558, 137–146. 10.1113/jphysiol.2004.064980.

Nomura, A., Shigemoto, R., Nakamura, Y., Okamoto, N., Mizuno, N., and Nakanishi, S. (1994). Developmentally regulated postsynaptic localization of a metabotropic glutamate receptor in rat rod bipolar cells. *Cell* 77, 361–369. 10.1016/0092-8674(94)90151-1.

O'Hare, F., Bentley, S.A., Wu, Z., Guymer, R.H., Luu, C.D., and Ayton, L.N. (2015). Charles Bonnet Syndrome in Advanced Retinitis Pigmentosa. *Ophthalmology* 122, 1951–1953. 10.1016/j.ophtha.2015.03.006.

Pang, J.J., Gao, F., and Wu, S.M. (2003). Light-evoked excitatory and inhibitory synaptic inputs to ON and OFF alpha ganglion cells in the mouse retina. *J Neurosci* 23, 6063–6073. 10.1523/JNEUROSCI.23-14-06063.2003.

Pang, J.J., Abd-El-Barr, M.M., Gao, F., Bramblett, D.E., Paul, D.L., and Wu, S.M. (2007). Relative contributions of rod and cone bipolar cell inputs to AII amacrine cell light responses in the mouse retina. *J Physiol* 580, 397–410. 10.1113/jphysiol.2006.120790.

Peachey, N.S., Ray, T.A., Florijn, R., Rowe, L.B., Sjoerdsma, T., Contreras-Alcantara, S., Baba, K., Tosini, G., Pozdeyev, N., Iuvone, P.M., *et al.* (2012). GPR179 is required for depolarizing bipolar cell function and is mutated in autosomal-recessive complete congenital stationary night blindness. *Am J Hum Genet* 90, 331–339. 10.1016/j.ajhg.2011.12.006.

Pinto, L.H., Vitaterna, M.H., Shimomura, K., Siepka, S.M., Balannik, V., McDearmon, E.L., Omura, C., Lumayag, S., Invergo, B.M., Glawe, B., *et al.* (2007). Generation, identification and functional characterization of the nob4 mutation of Grm6 in the mouse. *Vis Neurosci* 24, 111–123. 10.1017/S0952523807070149.

Prusky, G.T., Alam, N.M., Beekman, S., and Douglas, R.M. (2004). Rapid quantification of adult and developing mouse spatial vision using a virtual optomotor system. *Invest Ophthalmol Vis Sci* 45, 4611–4616. 10.1167/iovs.04-0541.

Ratnam, K., Carroll, J., Porco, T.C., Duncan, J.L., and Roorda, A. (2013). Relationship between foveal cone structure and clinical measures of visual function in patients

with inherited retinal degenerations. *Investigative Ophthalmology & Visual Science* 54(2), 583–592.

Robson, J.G., and Frishman, L.J. (2014). The rod-driven a-wave of the dark-adapted mammalian electroretinogram. *Prog Retin Eye Res* 39, 1–22. 10.1016/j.preteyeres.2013.12.003.

Rosa, J.M., Ruehle, S., Ding, H., and Lagnado, L. (2016). Crossover Inhibition Generates Sustained Visual Responses in the Inner Retina. *Neuron* 90, 308–319. 10.1016/j.neuron.2016.03.015.

Sawant, A., Ebbinghaus, B.N., Bleckert, A., Gamlin, C., Yu, W.Q., Berson, D., Rudolph, U., Sinha, R., and Hoon, M. (2021). Organization and emergence of a mixed GABA-glycine retinal circuit that provides inhibition to mouse ON-sustained alpha retinal ganglion cells. *Cell Rep* 34, 108858. 10.1016/j.celrep.2021.108858.

Scalabrino, M.L., Thapa, M., Wang, T., Sampath, A.P., Chen, J., and Field, G.D. (2023). Late gene therapy limits the restoration of retinal function in a mouse model of retinitis pigmentosa. *Nature Communications*, 14, 8256.

Scheiman, M., Mitchell, G.L., Cotter, S.A., Kulp, M.T., Cooper, J., Rouse, M.W., Hertle, R., Matta, N.S., and the Pediatric Eye Disease Investigator Group (2005). A randomized trial of treatment of amblyopia in children aged 7 to 17 years. *Archives of Ophthalmology* 123(4), 437–447.Schiller, P.H. (1982). Central connections of the retinal ON and OFF pathways. *Nature* 297, 580–583. 10.1038/297580a0.

Seiple, W., Holopigian, K., Szlyk, J. P., & Greenstein, V. C. (1995). The effects of random element loss on letter identification: implications for visual acuity loss in patients with retinitis pigmentosa. *Vision research*, *35*(14), 2057–2066.

Sinha, R., Grimes, W. N., Wallin, J., Ebbinghaus, B. N., Luu, K., Cherry, T., Rieke, F., Rudolph, U., Wong, R. O. and Hoon, M. (2021) Transient expression of a GABA receptor subunit during early development is critical for inhibitory synapse maturation and function, *Current Biology*, 31, 4314–4326.e5.

Sinha, R., Siddiqui, T. J., Padmanabhan, N., Wallin, J., Zhang, C., Karimi, B., Rieke, F., Craig, A. M., Wong, R. O. and Hoon, M. (2020) LRRTM4: A Novel Regulator of Presynaptic Inhibition and Ribbon Synapse Arrangements of Retinal Bipolar Cells, *Neuron*, 105, 1007–1017.e5.

Sinha, R., Hoon, M., Baudin, J., Okawa, H., Wong, R. O. L. and Rieke, F. (2017) Cellular and circuit mechanisms shaping the perceptual properties of the primate fovea, *Cell*, 168(3), pp. 413–426.e12.

Slaughter, M.M., and Miller, R.F. (1981). 2-amino-4-phosphonobutyric acid: a new pharmacological tool for retina research. *Science* 211, 182–185. 10.1126/science.6255566.

Smith, G. B. and Trachtenberg, J. T. (2007) Experience-dependent plasticity in the adult visual cortex: from synapses to networks, *Current Opinion in Neurobiology*, 17(3), 381–387.Stockton, R.A., and Slaughter, M.M. (1989). B-wave of the electroretinogram. A reflection of ON bipolar cell activity. *J Gen Physiol* 93, 101–122. 10.1085/jgp.93.1.101.

Turrigiano, G. (2011). Too many cooks? Intrinsic and synaptic homeostatic mechanisms in cortical circuit refinement. *Annu Rev Neurosci* 34, 89–103. 10.1146/annurev-neuro-060909-153238.

Turrigiano, G. (2012). Homeostatic synaptic plasticity: local and global mechanisms for stabilizing neuronal function. *Cold Spring Harb Perspect Biol* 4, a005736. 10.1101/cshperspect.a005736.

Turrigiano, G.G., Leslie, K.R., Desai, N.S., Rutherford, L.C., and Nelson, S.B. (1998). Activity-dependent scaling of quantal amplitude in neocortical neurons. *Nature* 391, 892–896. 10.1038/36103.

Van Genderen, M.M., Bijveld, M.M., Claassen, Y.B., Florijn, R.J., Pearring, J.N., Meire, F.M., McCall, M.A., Riemslag, F.C., Gregg, R.G., Bergen, A.A., and Kamermans, M. (2009). Mutations in TRPM1 are a common cause of complete congenital stationary night blindness. *Am J Hum Genet* 85, 730–736. 10.1016/j.ajhg.2009.10.012.

Van Boven, R. W., Hamilton, R. H., Kauffman, T., Keenan, J. P., & Pascual-Leone, A. (2000). Tactile spatial resolution in blind Braille readers. *Neurology, 54*(12), 2230–2236.

Vardi, N., Duvoisin, R., Wu, G., and Sterling, P. (2000). Localization of mGluR6 to dendrites of ON bipolar cells in primate retina. *J Comp Neurol* 423, 402–412. 10.1002/1096-9861(20000731)423:3<402::aid-cne4>3.0.co;2-e.

Verbakel, N., *et al.* (2018). [Details to be added]

Varin, J., Bouzidi, N., Gauvain, G., Joffrois, C., Desrosiers, M., Robert, C., De Sousa Dias, M.M., Neuille, M., Michiels, C., Nassisi, M., *et al.* (2021). Substantial restoration of night vision in adult mice with congenital stationary night blindness. *Mol Ther Methods Clin Dev* 22, 15–25. 10.1016/j.omtm.2021.05.008.

Vitureira, N., and Goda, Y. (2013). Cell biology in neuroscience: The interplay between Hebbian and homeostatic synaptic plasticity. *Journal of Cell Biology* **203**(2), 175–186. https://doi.org/10.1083/jcb.201306030.

Wan, C. Y., Wood, A.G., Reutens, D.C., & Wilson, S. J. (2010). Early but not late-blindness leads to enhanced auditory perception. *Neuropsychologia, 48*(1), 344–348.

Wassle, H. (2004). Parallel processing in the mammalian retina. *Nat Rev Neurosci* 5, 747–757. 10.1038/nrn1497.

Werblin, F.S., and Dowling, J.E. (1969). Organization of the retina of the mudpuppy, *Necturus maculosus*. II. Intracellular recording. *J Neurophysiol* 32, 339–355. 10.1152/jn.1969.32.3.339.

Wienbar, S., and Schwartz, G.W. (2022). Differences in spike generation instead of synaptic inputs determine the feature selectivity of two retinal cell types. *Neuron* 110, 2110–2123.e4. 10.1016/j.neuron.2022.04.012.

Wisner, S.R., Saha, A., Grimes, W.N., Mizerska, K., Kolarik, H.J., Wallin, J., Diamond, J.S., Sinha, R., and Hoon, M. (2023). Sensory deprivation arrests cellular and synaptic development of the night-vision circuitry in the retina. *Curr Biol* 33, 4415–4429.e13. 10.1016/j.cub.2023.08.087.

Wu, C. Y., Jansen, M.E., Andrade, J., Chui, T.Y.P., Do, A.T., Rosen, R.B. and Deobhakta, A. (2017) Acute solar retinopathy imaged with adaptive optics, optical coherence tomography angiography, and en face optical coherence tomography, *JAMA Ophthalmology*, 136(1), pp. 82–85. doi: 10.1001/jamaophthalmol.2017.5517.

Wu, K.Y., Kulbay, M., Toameh, D., Xu, A.Q., Kalevar, A. and Tran, S.D. (2023) Retinitis pigmentosa: novel therapeutic targets and drug development, *Pharmaceutics*, 15(2), 685. doi: 10.3390/pharmaceutics15020685.

Wynne, N., Carroll, J., & Duncan, J. L. (2021). Promises and pitfalls of evaluating photoreceptor-based retinal disease with adaptive optics scanning light ophthalmoscopy (AOSLO). *Progress in Retinal and Eye Research, 83*, 100920. https://doi.org/10.1016/j.preteyeres.2020.100920

Xu, H., Kotak, V.C., and Sanes, D.H. (2007). Conductive hearing loss disrupts synaptic and spike adaptation in developing auditory cortex. *J Neurosci* 27, 9417–9426. 10.1523/JNEUROSCI.1992-07.2007.

Yoon, B.J., Smith, G.B., Heynen, A.J., Neve, R.L., & Bear, M.F. (2009). Essential role for a long-term depression mechanism in ocular dominance plasticity. *Proc Natl Acad Sci* 106(23), 9860–9865. https://doi.org/10.1073/pnas.0902054106

Yoshida, K., Watanabe, D., Ishikane, H., Tachibana, M., Pastan, I., & Nakanishi, S. (2001). A key role of starburst amacrine cells in originating retinal directional selectivity and optokinetic eye movement. *Neuron*, *30*(4), 771–780. https://doi.org/10.1016/S0896-6273(01)00316-6

Yu, W.Q., El-Danaf, R.N., Okawa, H., Pacholec, J.M., Matti, U., Schwarz, K., Odermatt, B., Dunn, F.A., Lagnado, L., Schmitz, F., *et al.* (2018). Synaptic Convergence Patterns onto Retinal Ganglion Cells Are Preserved despite Topographic Variation in Pre- and Postsynaptic Territories. *Cell Rep* 25, 2017–2026.e13. 10.1016/j.celrep.2018.10.089.

Zaghloul, K.A., Boahen, K., and Demb, J.B. (2003). Different circuits for ON and OFF retinal ganglion cells cause different contrast sensitivities. *J Neurosci* 23, 2645–2654. 10.1523/JNEUROSCI.23-07-02645.2003.

Zeitz, C., Robson, A.G., and Audo, I. (2015). Congenital stationary night blindness: an analysis and update of genotype-phenotype correlations and pathogenic mechanisms. *Prog Retin Eye Res* 45, 58–110. 10.1016/j.preteyeres.2014.09.001.